A DESIGN PROGRAM FOR

SUPERCONDUCTING ELECTRICAL MACHINES

Author: David P. Greeneisen

Supervisor: H. H. Woodson
Professor of
Electrical Engineering

Submitted: 17 May, 1968

A DESIGN PROGRAM FOR SUPERCONDUCTING ELECTRICAL MACHINES

by

DAVID GREENEISEN

BS UNITED STATES NAVAL ACADEMY

(1963)

SUBMITTED TO THE DEPARTMENT OF NAVAL ARCHITECTURE AND MARINE ENGINEERING IN PARTIAL FULFILLMENT OF THE REQUIREMENTS OF THE MASTER OF SCIENCE DEGREE IN ELECTRICAL ENGINEERING AND THE PROFESSIONAL DEGREE, NAVAL ENGINEER

at the

MASSACHUSETTS INSTITUTE OF TECHNOLOGY

May, 1968

A DESIGN PROGRAM FOR

SUPERCONDUCTING ELECTRICAL MACHINES

by

DAVID GREENEISEN

ABSTRACT

Submitted to the Department of Naval Architecture and Marine Engineering on May 17, 1968 in partial fulfillment of the requirements for the Master of Science Degree in Electrical Engineering and the Professional Degree, Naval Engineer.

This paper presents a procedure for the design of superconducting electrical machines. The magnetostatic field problem of a cylindrical superconducting machine is solved. Equations for the magnetic fields are developed, and from these, expressions for the various machine parameters are obtained. These expressions are adapted to a computer solution of the design problem. The computer program obtains the design parameters for a minimum volume machine design.

A design study for a typical marine electrical propulsion system is conducted. The results of this study indicate quantitatively the reduction in weight and space to be obtained in using superconducting electrical machines vice conventional electrical machinery. The study also presents some general characteristics of superconducting machines.

Thesis Supervisor: H. H. Woodson
Title: Professor of Electrical Engineering

LIST OF FIGURES

LIST OF SYMBOLS

hp	Horsepower
kw	Kilowatts
l	Electrical length of windings
l_m	Effective length of windings for mutual inductance calculations
l_t	Total length of windings
p	Number of pole pairs
r	Radial dimension
t	Thickness
x	R_i/R_o
y	R_1/R_2
B	Magnetic flux density
H	Magnetic field intensity
I_a, I_f	Current in armature and field windings
J_a, J_f	Average current density in armature and field windings
K	Surface current density
L_a, L_f	Fundamental self-inductance of armature and field windings
M	Fundamental mutual inductance between armature and field windings
N_a, N_f	Number of turns in armature and field windings
P_g	Internally generated power
P_o	Power output

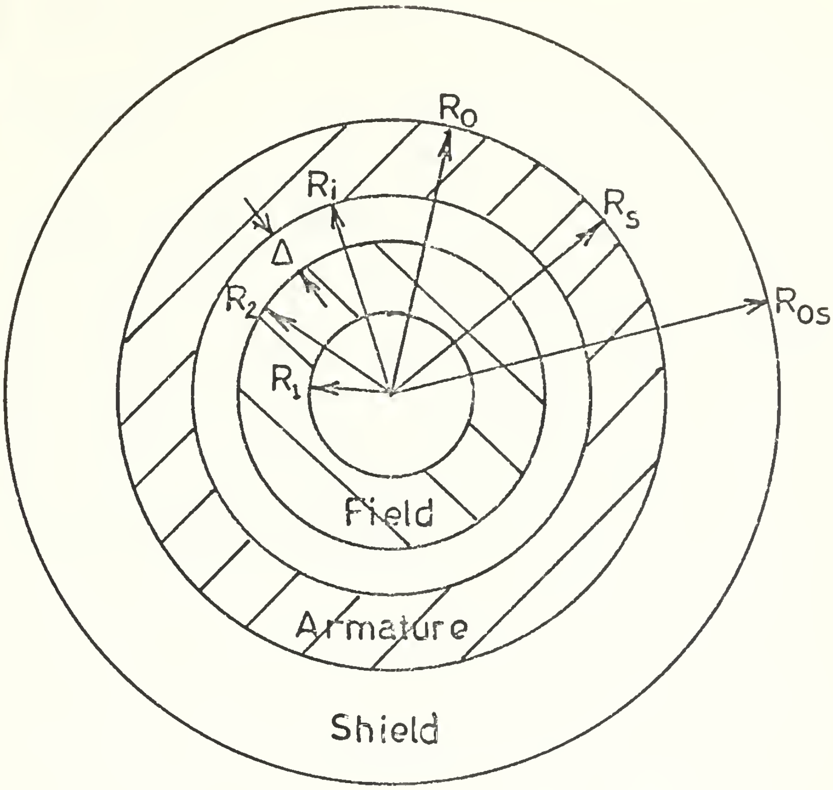

Figure 1 Machine cross section

R_{os}	Outside radius of shield
R_s	Inside radius of shield
R_o	Outside radius of armature
R_i	Inside radius of armature
R_2	Outside radius of field
R_1	Inside radius of field
Δ	$R_i - R_2$

λ	Flux linkage
δ	$\frac{R_i - R_2}{R_o}$
Θ	Power factor angle
μ_o	Permeability of free space
ω_e	Electrical angular velocity
ω_m	Mechanical angular velocity
ρ_f, ρ_a, ρ_s	Densities of material in field, armature and shield

ACKNOWLEDGEMENT

Any significance attaching to this paper results from the guidance of Professor H. H. Woodson, whose efforts made this exercise a meaningful learning experience.

TABLE OF CONTENTS

I. INTRODUCTION

A. Background

The relative flexibility and simplicity accruing to electrical power systems, in comparison to mechanical power systems, has long been recognized. Specifically, electrical power, and transmission systems provide flexibility of installation, are easily suited to automation and have a high degree of dependability.

Despite these advantages, and others that could be obtained, the full benefit of electrical power systems has not been realized in marine propulsion applications. To be sure, electric drive systems have been used in ship propulsion, however, such use has been mostly limited to small or intermediate size propulsion plants. The primary reason that electric drive systems have not been adopted for large power plants has been that the weight and space for such systems is greater than that required for geared propulsion systems. In addition, increased cost (as much as 20%) and lower efficiency (85% for DC) have been contributory factors(1)*

It is advantageous to consider some of the benefits that could be obtained with electric propulsion in order that aspects of its utilization might be judged in proper perspective.

As mentioned above, an electric propulsion system affords greater flexibility of installation. In constrast with a conventional geared propulsion system, extensive shafting is not

*Numbers in parentheses indicate applicable reference in the bibliography.

required and the location of the power source is not as restricted. In addition, the large, noisy reduction gear could be eliminated. The noise generated by this component is of increasing military significance.

If a cycloconverter* is used, additional benefits derive. It would be possible to use a constant frequency generator, thus permitting a more efficient design of the prime-mover. This will also permit greater use of newly developed power sources such as the gas turbine. Added to this would be more adaptation of remote and automatic controls, plus much improved maneuvering characteristics.(2,9)

Thus it seems that if the disadvantages (weight, space, and possibly efficiency) of electric propulsion are reduced, it will be given greater consideration as an alternative to geared propulsion in larger power systems.

B. The Role of Superconductors

It has been realized for some time that when the temperature of an electrical conductor is reduced to a few degrees absolute, the resistance of the conductor decreases to an unmeasurable amount. The implications of this fact have considerable value for use in electrical machines. If the resistance in the windings of an electrical generator or motor is removed, much greater current densities can be achieved with an accompanying increase in the magnetic flux densities within the machine.(3) If this

---

*An electronic power transmission device that affords changes in voltage and frequency. See reference 4.

increase in flux density is obtained, then greater power can be generated within a given volume. Thus it follows that the volume of an electric machine can be reduced if superconducting windings are used. Studies to date,[3] have demonstrated the significant reduction in volume and weight in superconducting machines.

However, the application of superconductivity is not without its complications. The first question which must be asked concerns the method of operating a machine wherein all, or at least some, of its parts are at a temperature in the region of liquid helium.

It is at this point convenient to limit the scope of the examination. The ensuing discussion will treat only machines with a rotating field winding, operating in the superconducting region, enclosed by a stationary armature at ambient temperature. This particular configuration is only one of several that could be considered.

There are two particular reasons why this configuration is selected. The more obvious is that it would be impractical to transfer the high machine power output through slip rings, as would be necessary if the armature were rotating. The other reason results from the fact that large heat losses are encountered when superconductors are subjected to alternating currents.[3] Thus, only the field winding is made superconducting.

Nonetheless, most of the techniques in this paper are generally applicable to any cylindrical electrical device.

With the discussion constrained to considering a rotating superconducting field winding, it is possible to dilineate some design procedure. Thus far, it has been found that the use of a thermal bottle, or dewar*, filled with liquid helium and encompassing the rotor, is a satisfactory solution to the problem of maintaining the windings in a superconducting state. Several techniques are under development for introducing the helium into the rotating dewar and passing electrical leads into the low-temperature region. Generally it is favorable to use the liquid helium dewar in conjunction with a liquid nitrogen dewar immediately exterior. The helium maintains the rotor at about $4.2^{\circ}K$ while the nitrogen offers a $77^{\circ}K$ buffer for improved cryogenic performance. At first, one might think that the refrigeration load for maintaining such low temperatures would be excessive. However, it should be realized that once the low temperatures are obtained, there is very little heat generated by the windings. Indeed, heat introduced into the low-temperature region through the shaft and support structure is more significant. A reasonable estimate of the power requirements for refrigeration during operation of a superconducting machine would be about 0.5 percent of rated power.(1)

In addition to the requirement that a superconductor be maintained at a low temperature, there is a limitation on the amount of current carried while exposed to a magnetic field. As indicated in Figure 2, if the magnetic flux density increases,

---

*Named after the inventor.

the permissible current density is reduced. If current or field exceed the limits imposed (the so-called critical values), the conductor reverts to its normal state. Thus it is necessary, in any particular machine design, to determine that combination of maximum flux density and current density which best suit the design.

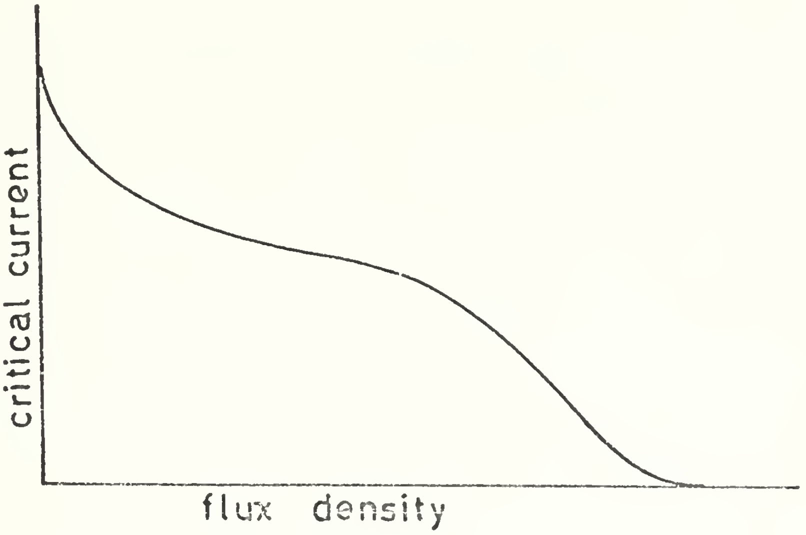

Figure 2 Current-Flux Relationship for a Typical Superconductor

The very fact that a superconducting machine develops extremely intense magnetic fields invites yet another complication. Since fields of the order of several kilo-gauss can be expected within the machine, disturbance of equipment in the vicinity of the machine will certainly result, as well as unbalanced loads on the superconducting field winding. Therefore, it is necessary that a shield be provided to confine the magnetic fields within the machine.

This shield would typically be of laminated steel construction and will be a significant portion of the size and weight of the machine.

C. Design Program

Though superconducting machines of the size suggested by the foregoing discussion have not yet been built, they are certainly feasible. Anticipating the construction of such machines, it is considered desirable to investigate some of their expected properties. Since there is vested interest in the reduced size and weight of these machines, it is natural that a design procedure be developed for obtaining minimum weight and volume.

The objective herein is to find a procedure for finding design characteristics of least size machines. The procedure developed is founded on a field-theory solution of the electric machine and is adapted to a computer solution.

II. PROCEDURE

A. Development of a Model

The first step in the analysis was to obtain a mathematical model for the magnetic fields involved. This model was necessary to determine the parameters which would be used in machine design. As mentioned previously, the model and attendant equations are for a rotating field winding inside a three-phase stator winding.

Analysis proceeded by considering both the field and stator windings to consist of cylindrical current sheets. Equations for the magnetic fields generated by each winding were developed separately and later combined to obtain necessary inductance and energy expressions.

To illustrate the analysis, consider the field windings. As illustrated in Figure 3, a cylindrical current sheet, $K(r)$, of thickness $d\rho$, located at some radius r, $R_1 < r < R_2$, is examined

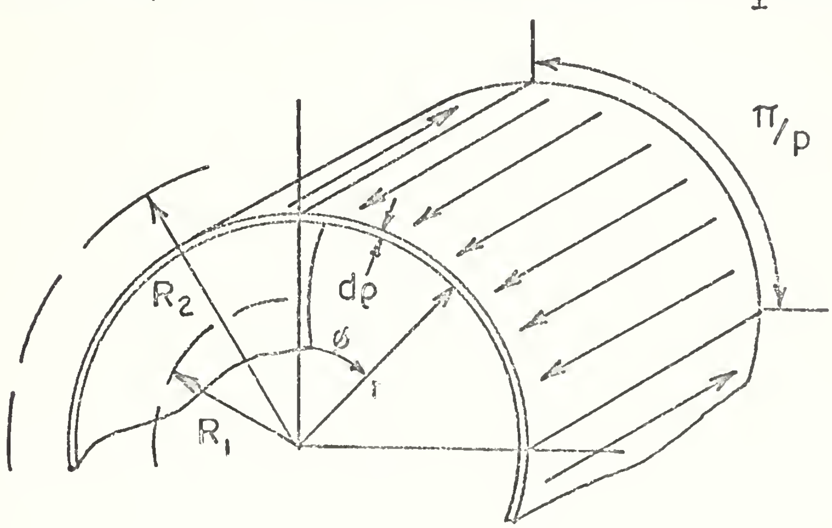

Figure 3 Distribution of Current Sheet $K(r)$

Fourier analysis of this current sheet yields:

$$K(r) = \sum_{n \text{ odd}} \frac{4J_f dr}{n\pi} \sin np\phi . \qquad \text{(II-1)}$$

Knowing that these current sheets exist between $r = R_1$ and $r = R_2$, and that the fields associated with each sheet are Laplacian, enables determination of the field expressions.(5) After finding an expression for the magnetic field for $r \geq R_2$, one can find the contribution due to the shield. Since at $r = R_s$, with an infinitely permeable shield,

$$H_{s\phi} = -H_{f\phi} \qquad \text{(II-2)}$$

and at $r = 0$,

$$H_{s\rho} = \text{finite} \qquad \text{(II-3)}$$

an expression is found for the fields induced by the shield. The expression thus obtained is then added to that for the fields generated by the field winding.

This same procedure obtains for determining the magnetic field system resulting from the armature windings. The only difference involved is in the current sheet model used, since the armature is a three-phase winding, with 60-degree phase belts.

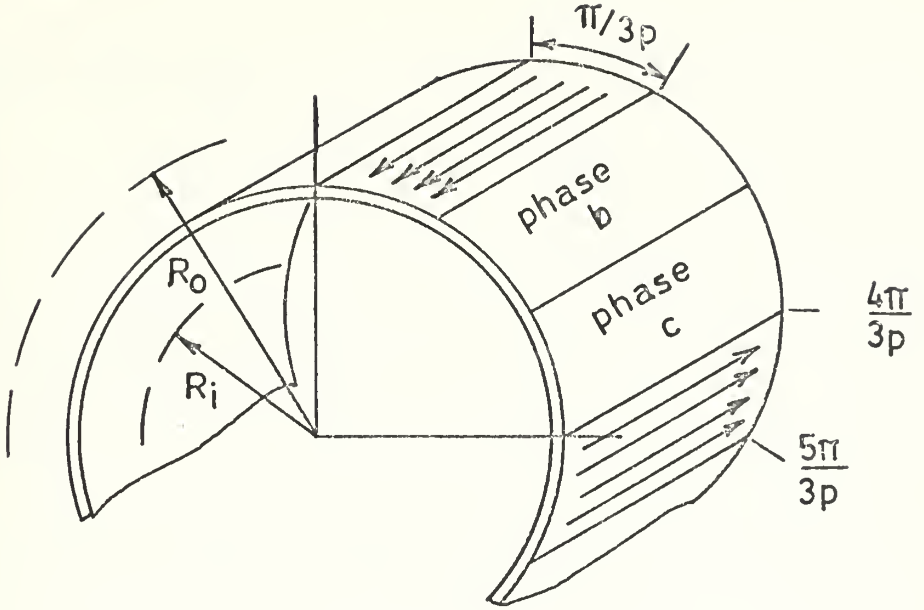

Figure 4   Distribution of Armature Current Sheet

Fourier analysis of the armature current sheet yields

$$K_a(r) = \sum_{n \text{ odd}} \frac{4J_a dr}{n\pi} \cos\frac{n\pi}{3} \sin np\phi \,. \tag{II-4}$$

Expressions for magnetic field systems of the field and armature windings are presented in Tables 1 and 2.

Using the equations for the magnetic fields, an expression for energy stored in the armature field system is obtained from

$$W_a = \int_0^{2\pi} \int_0^{Rs} \frac{1}{2}\mu_c \left(H_{a\rho}^2 + H_{a\phi}^2\right) l\rho \, d\rho \, d\phi \,. \tag{II-5}$$

Equating the result in

$$W_a = \frac{1}{2} L_a I_a^2, \tag{II-6}$$

where

$$I_a = \frac{\pi(R_o^2 - R_i^2)\ J_a}{6\ N_a}, \tag{II-7}$$

yields an expression for the armature self-inductance. A similar calculation is performed to obtain the field winding self-inductance.

Mutual inductance is found from

$$I_f L_{af} = \lambda, \tag{II-8}$$

where λ is the total field-winding flux linkage of the armature windings. By recognizing that $6N_a/\pi(R_o^2 - R_i^2)$ expresses the number of armature turns per unit cross-section, then the second spatial differential of the flux linkage is expressed by

$$d^2\lambda = \frac{6N_a}{\pi(R_o^2 - R_i^2)}\ \mu_o\, \rho\, d\rho\ d\phi \int_{\phi - \frac{\pi}{p}}^{\phi} H_{f\rho}\ l d\rho\ d\psi. \tag{II-9}$$

TABLE 1

Magnetic Field Equations for Field Windings

$$np \neq 2$$

$\rho < R_1$

$$H_\rho = \sum_{n\ \mathrm{odd}} \frac{2J_f}{n\pi(2-np)} \left(R_2^{-np+2} - R_1^{-np+2}\right) \rho^{np-1} \cos np\phi$$

$$\times \left[1 + \frac{2-np}{2+np} \, \frac{R_2^{np+2} - R_1^{np+2}}{R_2^{-np+2} - R_1^{-np+2}} \, \frac{1}{R_s^{2np}}\right]$$

$$H_\phi = \sum_{n\ \mathrm{odd}} \frac{-2J_f}{\pi(2-np)} \left(R_2^{-np+2} - R_1^{-np+2}\right) \rho^{np-1} \sin np\phi$$

$$\times \left[1 + \frac{2-np}{2+np} \, \frac{R_2^{np+2} - R_1^{np+2}}{R_2^{-np+2} - R_1^{-np+2}} \, \frac{1}{R_s^{2np}}\right]$$

$R_1 < \rho < R_2$

$$H_\rho = \sum_{n\ \mathrm{odd}} \frac{2J_f}{n\pi(4-n^2p^2)} \, \rho \cos np\phi \left[-2np + (2+np)\left(\frac{R_2}{\rho}\right)^{-np+2} \right.$$

$$\left. - (2-np)\left(\frac{R_1}{\rho}\right)^{np+2} + (2-np) \, \frac{R_2^{np+2} - R_1^{np+2}}{R_s^{2np}} \, \rho^{np-2}\right]$$

$$H_\phi = \sum_{n\ \mathrm{odd}} \frac{2J_f}{\pi(4-n^2p^2)} \, [illegible] \sin np\phi \left[[illegible] - ([illegible])\left(\frac{R_2}{\rho}\right)^{-np+2} \right.$$

$$\left. - (2-np)\left(\frac{R_1}{\rho}\right)^{np+2} - (2-np) \, \frac{[illegible]}{[illegible]} \, \rho^{[illegible]}\right]$$

$\underline{R_2 < \rho < R_s}$

$$H_\rho = \sum_{n\ \mathrm{odd}} \frac{2J_f}{n\pi(2+np)} \left(R_2^{np+2} - R_1^{np+2}\right) \left[\rho^{-np-1} + \frac{\rho^{np-1}}{R_s^{2np}}\right] \cos np\phi$$

$$H_\phi = \sum_{n\ \mathrm{odd}} \frac{2J_f}{n\pi(2+np)} \left(R_2^{np+2} - R_1^{np+2}\right) \left[\rho^{-np-1} - \frac{\rho^{np-1}}{R_s^{2np}}\right] \sin np\phi$$

$\underline{np = 2}$ $(n=1,\ p=2)$

$\underline{\rho < R_1}$

$$H_\rho = \frac{2J_f}{\pi} \ln \frac{R_2}{R_1} \left[1 + \frac{1}{4} \frac{R_2^4 - R_1^4}{R_s^4 \ln(R_2/R_1)}\right] \rho \cos 2\phi$$

$$H_\phi = -\frac{2J_f}{\pi} \ln \frac{R_2}{R_1} \left[1 + \frac{1}{4} \frac{R_2 - R_1}{R_s^4 \ln(R_2/R_1)}\right] \rho \sin 2\phi$$

$\underline{R_1 < \rho < R_2}$

$$H_\rho = \frac{2J_f}{\pi} \left[\frac{1}{4}\left(1 - \frac{R_1}{\rho^4}\right) + \ln \frac{R_2}{\rho} + \frac{R_2^4 - R_1^4}{4R_s^4}\right] \rho \cos 2\phi$$

$$H_\phi = \frac{2J_f}{\pi} \left[\frac{1}{4}\left(1 - \frac{R_1}{\rho^4}\right) - \ln \frac{R_2}{\rho} - \frac{R_2^4 - R_1^4}{4R_s^4}\right] \rho \sin 2\phi$$

$\underline{R_2 < \rho < R_s}$

$$H_\rho = \frac{J_f}{2\pi} \left(R_2^4 - R_1^4\right) \left[\rho^{-3} + \frac{\rho}{R_s^4}\right] \cos 2\phi$$

$$H_\phi = \frac{J_f}{2\pi} \left(R_2^4 - R_1^4\right) \left[\rho^{-3} - \frac{\rho}{R_s^4}\right] \sin 2\phi$$

TABLE 2

Magnetic Field Equations for

Phase A of Armature Windings

$np \neq 2$

$\rho < R_i$

$$H_\rho = \sum_{n\ odd} \frac{2J_a \cos(n\pi/3)}{n\pi(2-np)} (R_o^{-np+2} - R_i^{-np+2})\, \rho^{np-1} \cos np\phi$$

$$\times \left[1 + \frac{2-np}{2+np} \frac{R_o^{np+2} - R_i^{np+2}}{R_o^{-np+2} - R_i^{-np+2}} \frac{1}{R_s^{2np}} \right]$$

$$H_\phi = \sum_{n\ odd} \frac{2J_a \cos(n\pi/3)}{n\pi(2-np)} (R^{-np+2} - R^{-np+2})\, \rho^{np-1} \sin np\phi$$

$$\times \left[1 + \frac{2-np}{2+np} \frac{R_o^{np+2} - R_i^{np+2}}{R_o^{-np+2} - R_i^{-np+2}} \frac{1}{R_s^{2np}} \right]$$

$R_i < \rho < R_o$

$$H_\rho = \sum_{n\ odd} \frac{2J_a \cos(n\pi/3)}{n\pi(4-n^2p^2)}\, \rho \cos np\phi \left[-2np + (2+np)\left(\frac{R_o}{\rho}\right)^{-np+2} \right.$$

$$\left. - (2-np)\left(\frac{R_i}{\rho}\right)^{np+2} + (2-np)\frac{R_o^{np+2} - R_i^{np+2}}{R_s^{2np}}\, \rho^{np-2} \right]$$

$$H_\phi = \sum_{n\ odd} \frac{2J_a \cos(n\pi/3)}{n\pi(4-n^2p^2)}\, \rho \sin np\phi \left[4 - (2+np)\left(\frac{R_o}{\rho}\right)^{-np+2} \right.$$

$$\left. - (2-np)\left(\frac{R_i}{\rho}\right)^{np+2} - (2-np)\frac{R_o^{np+2} - R_i^{np+2}}{R_s^{2np}}\, \rho^{np-2} \right]$$

$R_o < \rho < R_s$

$$H_\rho = \sum_{n\ \mathrm{odd}} \frac{2J_a \cos(n\pi/3)}{n\pi(2+np)} \left(R_o^{np+2} - R_i^{np+2}\right)\left[\rho^{-np-1} + \frac{\rho^{np-1}}{R_s^{2np}}\right] \cos np\phi$$

$$H_\phi = \sum_{n\ \mathrm{odd}} \frac{2J_a \cos(n\pi/3)}{n\pi(2+np)} \left(R_o^{np+2} - R_i^{np+2}\right)\left[\rho^{-np-1} - \frac{\rho^{np-1}}{R_s^{2np}}\right] \sin np\phi$$

$np = 2$ $(n=1,\ p=2)$

$\rho < R_i$

$$H_\rho = \frac{J_a}{\pi} \ln \frac{R_o}{R_i} \left[1 + \frac{1}{4}\,\frac{R_o^4 - R_i^4}{R_s^4 \ln(R_o/R_i)}\right] \rho \cos 2\phi$$

$$H_\phi = -\frac{J_a}{\pi} \ln \frac{R_o}{R} \left[1 + \frac{1}{4}\,\frac{R_o^4 - R_i^4}{R_s^4 \ln(R_o/R_i)}\right] \rho \sin 2\phi$$

$R_i < \rho < R_o$

$$H_\rho = \frac{J_a}{\pi}\left[\frac{1}{4}\left(1 - \frac{R_i}{\rho^4}\right) + \ln\frac{R_o}{\rho} + \frac{R_o - R_i}{4R_s^4}\right] \rho \cos 2\phi$$

$$H_\phi = \frac{J_a}{\pi}\left[\frac{1}{4}\left(1 - \frac{R_i}{\rho^4}\right) - \ln\frac{R_o}{\rho} - \frac{R_o - R_i}{4R_s^4}\right] \rho \sin 2\phi$$

$R_o < \rho < R_s$

$$H_\rho = \frac{J_a}{4\pi}\left(R_o^4 - R_i^4\right)\left[\rho^{-3} + \frac{\rho}{R_s^4}\right] \cos 2\phi$$

$$H_\phi = \frac{J_a}{4\pi}\left(R_o^4 - R_i^4\right)\left[\rho^{-3} - \frac{\rho}{R_s^4}\right] \sin 2\phi$$

Integrating this expression over the cross-section of the armature yields the total flux linkage and thus the mutual inductance. Expressions for field and armature self-inductance and mutual inductance are presented in Table 3.

B. Design Equations

If one considers the amplitudes of the line-to-neutral armature voltage and armature current, one obtains

$$V_a = \omega_e M I_f, \tag{II-10}$$

$$I_a = \frac{\pi(R_o^2 - R_i^2)J_a}{6N_a}, \tag{II-11}$$

$$P_g = \frac{3}{2}V_a I_a, \tag{II-12}$$

where

$$I_f = \frac{\pi(R_2^2 - R_1^2)J_f}{2N_f}. \tag{II-13}$$

This power is internally generated power, which must be reduced, to account for armature impedance and the load power factor, in order to obtain rated output power.

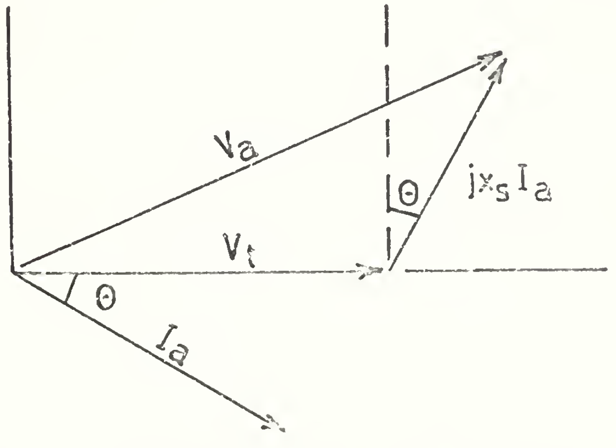

Figure 5 Vector Diagram of Generator Voltages

TABLE 3

Inductance Equations

$$p \neq 2$$

$$L_f = \frac{16\mu_0 N_f^2 l}{\pi^3 p(p^2-4)(1-y^2)^2}\left[(p-2) - (p+2)y^4 + 4y^{p+2} + 2\frac{p-2}{p+2}(1-y^{p+2})\left(\frac{R_2}{R_s}\right)^{2p}\right]$$

$$L_a = \frac{16\mu_0 N_a^2 l}{\pi^3 p(p^2-4)(1-x^2)^2}\left[(p-2) - (p+2)x^4 + 4x^{p+2} + 2\frac{p-2}{p+2}(1-x^{p+2})\left(\frac{R_2}{R_s}\right)^{2p}\right]$$

$$M = \frac{48\mu_0 N_a N_f l(1-y^{p+2})}{\pi^3 p(1-x^2)(1-y^2)}\left(\frac{R_2}{R_o}\right)^p\left[\frac{1-x^{-p+2}}{4-p^2} + \frac{1-x^{p+2}}{(2+p)^2}\left(\frac{R_o}{R_s}\right)^{2p}\right]$$

$$p = 2$$

$$L_f = \frac{8\mu_0 N_f^2 l}{\pi^3(1-y^2)^2}\left[\frac{1}{4}(1-y^4) + y^4 \ln y + \frac{1}{8}(1-y^4)^2\left(\frac{R_2}{R_s}\right)^{2p}\right]$$

$$L_a = \frac{18\mu_0 N_a l}{\pi^3(1-x^2)^2}\left[\frac{1}{4}(1-x^4) + x^4 \ln x + \frac{1}{8}(1-x^4)^2\left(\frac{R_o}{R_s}\right)^{2p}\right]$$

$$M = \frac{6\mu_0 N_a N_f l(1+y^2)}{\pi^3(1-x^2)}\left(\frac{R_2}{R_o}\right)^2\left[\ln\frac{1}{x} + \frac{(1-x^4)}{4}\left(\frac{R_o}{R_s}\right)^{2p}\right]$$

From the vector diagram in Figure 5, where

$$x_s = \omega_e L_a, \tag{II-14}$$

the ratio V_t/V_a is obtained. Then rated power is

$$P = P_g(V_t/V_a)\cos\theta. \tag{II-15}$$

In developing the equations describing the machine, some approximation was necessary to account for the effects of the end-turns.[10] Figure 6 shows the geometry involved in making this approximation.

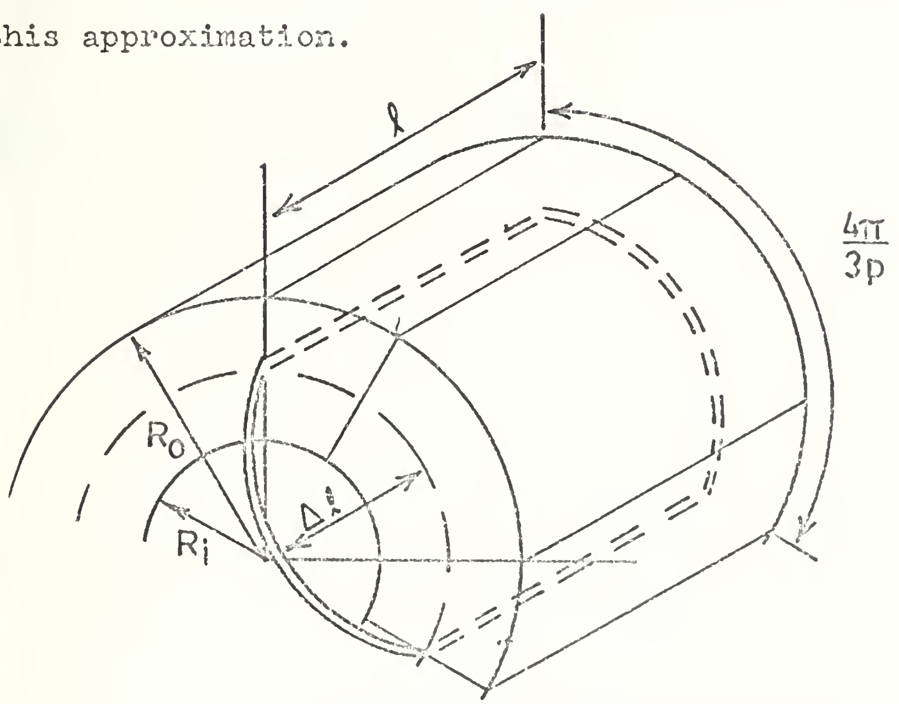

Figure 6 End-Turn Geometry

If one considers an outer armature turn at the mean radius of a given phase winding, it is seen that the angular displacement

of this coil is $4\pi/3p$ radians. Since this coil is at a radius

$$r = \frac{1}{2}(R_o + R_i) \tag{II-16}$$

the approximation can be made that

$$\Delta l = \frac{1}{2} \cdot \frac{4\pi}{3p} \cdot \frac{1}{2}(R_o + R_i) = \frac{\pi}{3p}(R_o + R_i). \tag{II-17}$$

Using this expression, it has been found[6] that a reasonable length to assume for self-inductance calculations is the total length

$$l_t = l + 2\Delta l, \tag{II-18}$$

whereas the length to be used for mutual inductance is

$$l_m = l + \Delta l. \tag{II-19}$$

C. <u>Design Limitations</u>

As described in the Introduction, the low resistance character of a superconducting coil is not only a function of temperature, but also depends on its current density and the magnetic field to which it is exposed. Thus for a given design it is necessary to determine the maximum magnetic flux density associated with any particular current density, to ensure that the superconducting field winding will not revert to its normal state. The particular mechanics employed to observe this

limitation are detailed in the program construction techniques of Appendix C.

As also mentioned in the Introduction, the machine design considered employs a shield (constructed of laminated steel) which contains the dense magnetic fields within the machine. For this shield to be effective, the fields it constrains must be less than those which will cause saturation of the shield. If the shield material saturates at some density B_{rated}, then one limitation is

$$B_{max.}(r = R_o) \leq B_{rated}. \tag{II-20}$$

Another limitation exists in the requirement that the maximum flux density carried by the shield must never exceed B_{rated}. As illustrated in

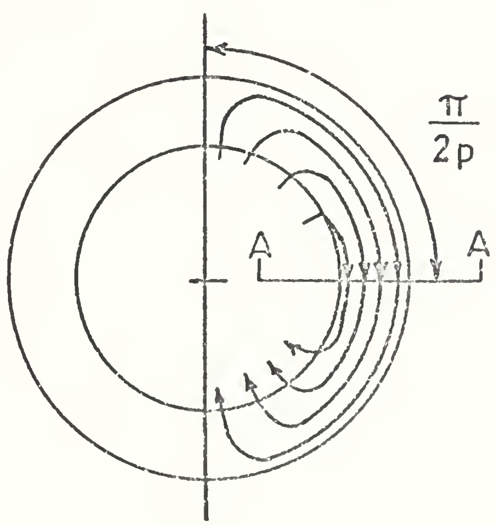

Figure 7 Shield Flux Pattern

Figure 7, the total flux accumulated by the shield over an angle of $\pi/2p$ must not be sufficient to cause saturation in the cross-

section at A-A. Since

$$\Phi_{A-A} = \int_0^{\pi/2p} B_\rho (R_o) l R_o d\phi , \qquad \text{(II-21)}$$

a final constraint is obtained in

$$\Phi_{A-A} \leq B_{rated} (R_{os} - R_o) l_t . \qquad \text{(II-22)}$$

There are two final considerations which may govern a machine design. First, the heat dissipation in the armature winding must be considered. Generally the maximum permissible current will be determined from the limitations imposed by the method adopted for cooling the armature. For purposes of this design it was assumed that an average armature current density of 1.6×10^6 amp/m^2 could be accepted with chilled water cooling of the winding. Finally, one must consider the speed of the machine rotating parts. The strength of the rotor structure will provide a limit to the rotor tip speed that can be sustained. On consideration of previous conventional machine design it was determined that 700 ft/sec was a reasonable upper value for tip speed. However, since methods of constructing superconducting windings are far from being fixed, this value for maximum tip speed is speculative. The tip speed of the rotor will also be governed by the performance of the rotating dewar. In this respect, the fluidic and thermodynamic properties of liquid helium, under high centrifugal forces, will govern. Since the

aspects of this consideration are yet to be determined, it is assumed here that the previously stated maximum tip speed is acceptable.

III. RESULTS

The significance of this work lies in the results of a design study which was conducted, employing the design procedure described in Part II. The design study involved what was considered a typical marine electrical propulsion system; a turbine driven generator rated at 26 MW (35,000 hp) at 3600 rpm, and two direct drive propulsion motors rated at 17,500 bhp (13 MW) at 300 rpm. Other parameters assumed were:

$J_f = 1.0 \times 10^8$ amp/m^2

$J_a = 1.6 \times 10^6$ amp/m^2

$B_{max} = 5.0$ web/m^2

$B_{rated} = 2.0$ web/m^2

$\rho_f = 4000$ kg/m^3

$\rho_a = 4000$ kg/m^3
(copper with .45 packing factor)

$\rho_s = 8000$ kg/m^3
(steel)

$\delta = .05$m

Tip speeds of up to 214 m/sec (700 ft/sec) were considered in both the generator and motor designs. Also, for the generator, designs with power factors of 1.0, .850 and .707 were examined. Design characteristics of machines with 1 to 6 pole pairs were computed for all variations.

The computer results and graphs of the characteristics of some of the more interesting designs are included in the following pages.

One quantity, not calculated by the computer program, that should be examined is the machine efficiency.

Since

$$R_a = \frac{\rho_r N_a l_t}{A_x} \qquad \text{(III-1)}$$

where ρ_r = resistivity = 1.9×10^{-8} ohm-m and cross-section area is

$$A_x = \frac{\pi(1-x^2)R_o^2 \cdot .45}{6N_a}, \qquad \text{(III-2)}$$

for a .45 packing factor, then for the optimum generator design (pf = .707, p = 6, V_{tip} = 214 m/sec)

$$R_a/N_a^2 = 6.7 \times 10^{-8} \text{ ohm/turn}^2.$$

Knowing $N_a I_a$, it is possible to find

$$I_a^2 R_a = 965 \text{ watts.}$$

These losses, however, are for only one phase and were computed with a peak value for I_a instead of rms. Therefore, resistive losses for all three phases are

$$I_a^2 R_a = 965 \cdot \frac{3}{2} = 1450 \text{ watts.}$$

If an equal amount is allowed for eddy current losses, a figure of 2900 watts is obtained for the total losses. Since this is for a 26 MW generator, this loss will cause a negligible reduction in efficiency.

DATA P = 4

DELTA = 0.050 M JF = 0.10E 09 A/M2 OMEGA = 377. RAD/SEC

PAR = 26.0 MW JA = 0.16E 07 A/M2 FLD DENSS = 4000. KG/M3

VTIP = 122. M/SEC B MAX = 5.0 WEB/M2 ARM DENSS = 4000. KG/M3

PF ANG = 0.784 RAD B RATED = 2.0 WEB/ M2 SHL DENSS = 8000. KG/M3

DESIGN PARAMETERS

X	Y	RO (M)	ROS (M)	LT (M)	XA (P.U.)	VT/N (V/TURN)	NIA (A-TURNS)	POUT (MW)	VOL (M3)	WGT (KG)	VI (MW)
.931	0.675	0.347	0.434	3.958	0.012	1900.	0.13E 05	25.7	2.345	9574.	36.7
.809	0.675	0.399	0.449	2.116	0.057	585.	0.46E 05	25.9	1.343	4786.	38.1
.647	0.675	0.499	0.520	1.823	0.235	232.	0.12E 06	25.9	1.550	5206.	43.2
.539	0.675	0.599	0.609	2.120	0.705	130.	0.21E 06	25.7	2.476	8515.	57.5
.462	0.675	0.399	0.705	4.285	3.046	81.	0.32E 06	26.0	6.697	23739.	140.5

MINIMUM VOLUME DESIGN

X	Y	RO (M)	ROS (M)	LT (M)	XA (P.U.)	VT/N (V/TURN)	NIA (A-TURNS)	POUT (MW)	VOL (M3)	WGT (KG)	VI (MW)
.719	0.675	0.455	0.484	1.836	0.136	322.	0.86E 05	25.8	1.356	4587.	40.1

DATA P = 5

DELTA = 0.050 M JF = 0.10E 09 A/M2 OMEGA = 377. RAD/SEC

PWR = 26.0 MW JA = 0.16E 07 A/M2 FLD DENSS = 4000. KG/M3

VTIP = 153. M/SEC B MAX = 5.0 WEB/M2 ARM DENSS = 4000. KG/M3

PF ANG = 0.784 RAD B RATED = 2.0 WEB/ M2 SHL DENSS = 8000. KG/M3

DESIGN PARAMETERS

X	Y	RO (M)	ROS (M)	LT (M)	XA (P.U.)	VT/N (V/TURN)	NIA (A-TURNS)	POUT (MW)	VOL (M3)	WGT (KG)	VI (MW)
.926	0.759	0.437	0.525	2.042	0.016	1189.	0.22E 05	25.9	1.772	6406.	37.1
.811	0.759	0.500	0.545	1.323	0.072	410.	0.71E 05	25.9	1.235	3881.	38.5
.676	0.759	0.600	0.618	1.263	0.250	187.	0.16E 06	26.0	1.516	4655.	43.6
.579	0.759	0.699	0.708	1.466	0.672	110.	0.27E 06	25.8	2.311	7417.	56.6
.507	0.759	0.799	0.804	2.348	2.176	69.	0.39E 06	25.9	4.773	16021.	103.6

MINIMUM VOLUME DESIGN

.773	0.759	0.524	0.560	1.268	0.103	321.	0.92E 05	25.8	1.250	3846.	39.3

DATA P = 6

DELTA = 0.050 M JF = 0.10E 09 A/M2 OMEGA = 377. RAD/SEC

PWR = 26.0 MW JA = 0.16E 07 A/M2 FLD DENSS = 4000. KG/M3

VTIP = 214. M/SEC B MAX = 5.0 WEB/M2 ARM DENSS = 4000. KG/M3

PF ANG = 0.784 RAD B RATED = 2.0 WEB/ M2 SHL DENSS = 8000. KG/M3

DESIGN PARAMETERS

X	Y	RO (M)	ROS (M)	LT (M)	XA (P.U.)	VT/N (V/TURN)	NIA (A-TURNS)	POUT (MW)	VOL (M3)	WGT (KG)	VI (MW)
.906	0.848	0.626	0.730	0.863	0.032	610.	0.58E 05	25.9	1.449	4657.	37.5
.810	0.848	0.699	0.753	0.763	0.104	292.	0.14E 06	25.8	1.362	3830.	39.3
.709	0.848	0.799	0.824	0.790	0.280	162.	0.26E 06	26.0	1.685	4681.	44.6
.630	0.848	0.899	0.911	0.879	0.634	101.	0.40E 06	25.9	2.296	6699.	55.6
.567	0.848	0.999	1.006	1.095	1.497	65.	0.56E 06	26.2	3.485	10719.	85.6

MINIMUM VOLUME DESIGN

.822	0.848	0.689	0.748	0.766	0.092	316.	0.12E 06	25.9	1.349	3830.	39.0

DATA P = 3

DELTA = 0.050 M JF = 0.10E 09 A/M2 OMEGA = 21. RAD/SEC

POUT = 13.0 KW JA = 0.16E 07 A/M2 FLD DENSS = 4000. KG/M3

VTIP = 8. M/SEC B MAX = 5.0 WEB/M2 ARM DENSS = 4000. KG/M3

DEF ANG = 0.000 RAD B RATED = 2.0 WEB/ M2 SHL DENSS = 8000. KG/M3

DESIGN PARAMETERS

X	Y	RO (M)	ROS (M)	LT (M)	XA (P.U.)	VT/N (V/TURN)	NIA (A-TURNS)	POUT (MW)	VOL (M3)	WGT (KG)	VI (MW)
.824	0.776	0.462	0.516	4.469	0.034	162.	0.57E 05	12.9	5.330	24940.	13.0
.761	0.776	0.500	0.621	3.682	0.058	108.	0.87E 05	12.9	4.469	19483.	13.0
.634	0.776	0.600	0.670	2.960	0.152	55.	0.18E 06	12.9	4.179	16262.	13.1
.544	0.776	0.699	0.744	2.768	0.310	35.	0.28E 06	12.9	4.818	17963.	13.5
.476	0.776	0.799	0.829	2.852	0.588	25.	0.41E 06	13.0	6.169	22767.	15.0
.423	0.776	0.899	0.920	3.523	1.250	18.	0.55E 06	13.0	9.387	34729.	20.9

MINIMUM VOLUME DESIGN

X	Y	RO (M)	ROS (M)	LT (M)	XA (P.U.)	VT/N (V/TURN)	NIA (A-TURNS)	POUT (MW)	VOL (M3)	WGT (KG)	VI (MW)
.652	0.776	0.583	0.660	3.002	0.134	59.	0.16E 06	12.8	4.112	16197.	13.0

DATA P = 5

DELTA = 0.050 M JF = 0.10E 09 A/M2 OMEGA = 21. RAD/SEC

PWR = 13.0 MW JA = 0.16E 07 A/M2 FLD DENSS = 4000. KG/M3

VTIP = 10. M/SEC B MAX = 5.0 WEB/M2 ARM DENSS = 4000. KG/M3

PF ANG = 0.000 RAD B RATED = 2.0 WEB/ M2 SHL DENSS = 8000. KG/M3

DESIGN PARAMETERS

X	Y	RO (M)	ROS (M)	LT (M)	XA (P.U.)	VT/N (V/TURN)	NIA (A-TURNS)	POUT (MW)	VOL (M3)	WGT (KG)	VI (MW)
.597	0.813	0.530	0.636	4.653	0.023	197.	0.45E 05	12.9	5.928	21299.	13.0
.793	0.813	0.600	0.657	3.235	0.071	83.	0.11E 06	12.9	4.392	13792.	13.0
.68[illegible]	0.813	0.699	0.726	2.837	0.183	43.	0.22E 06	12.9	4.705	14283.	13.2
.59[illegible]	0.813	0.799	0.813	2.801	0.369	27.	0.34E 06	12.9	5.825	18261.	13.8
.529	0.813	0.899	0.907	3.094	0.717	19.	0.48E 06	13.0	8.008	26140.	16.0

MINIMUM VOLUME DESIGN

X	Y	RO (M)	ROS (M)	LT (M)	XA (P.U.)	VT/N (V/TURN)	NIA (A-TURNS)	POUT (MW)	VOL (M3)	WGT (KG)	VI (MW)
.744	0.813	0.559	0.581	2.989	0.109	61.	0.15E 06	12.9	4.359	13302.	13.0

DATA P = 6

DELTA = 0.050 M JF = 0.10E 09 A/M2 OMEGA = 21. RAD/SEC

P.R = 13.0 MW JA = 0.16E 07 A/M2 FLD DENSS = 4000. KG/M3

VTIP = 15. M/SEC B MAX = 5.0 WEB/M2 ARM DENSS = 4000. KG/M3

PF ANG = 0.000 RAD B RATED = 2.0 WEB/ M2 SHL DENSS = 8000. KG/M3

DESIGN PARAMETERS

X	Y	RO (M)	ROS (M)	LT (M)	XA (P.U.)	VT/N (V/TURN)	NIA (A-TURNS)	POUT (MW)	VOL (M3)	WGT (KG)	VI (MW)
.879	0.887	0.812	0.947	1.505	0.042	88.	0.12E 06	12.9	4.243	13595.	13.0
.793	0.887	0.899	0.972	1.312	0.105	47.	0.25E 06	12.9	3.903	10994.	13.0
.714	0.887	0.999	1.038	1.283	0.211	30.	0.41E 06	12.9	4.349	11954.	13.2
.649	0.887	1.099	1.121	1.308	0.369	21.	0.58E 06	12.9	5.174	14644.	13.8
.595	0.887	1.195	1.212	1.392	0.616	16.	0.77E 06	13.0	6.437	19005.	15.2

MINIMUM VOLUME DESIGN

X	Y	RO (M)	ROS (M)	LT (M)	XA (P.U.)	VT/N (V/TURN)	NIA (A-TURNS)	POUT (MW)	VOL (M3)	WGT (KG)	VI (MW)
.801	0.887	0.891	0.968	1.320	0.098	49.	0.23E 06	12.9	3.893	11044.	13.0

Figure 8
Generator Specific Weight

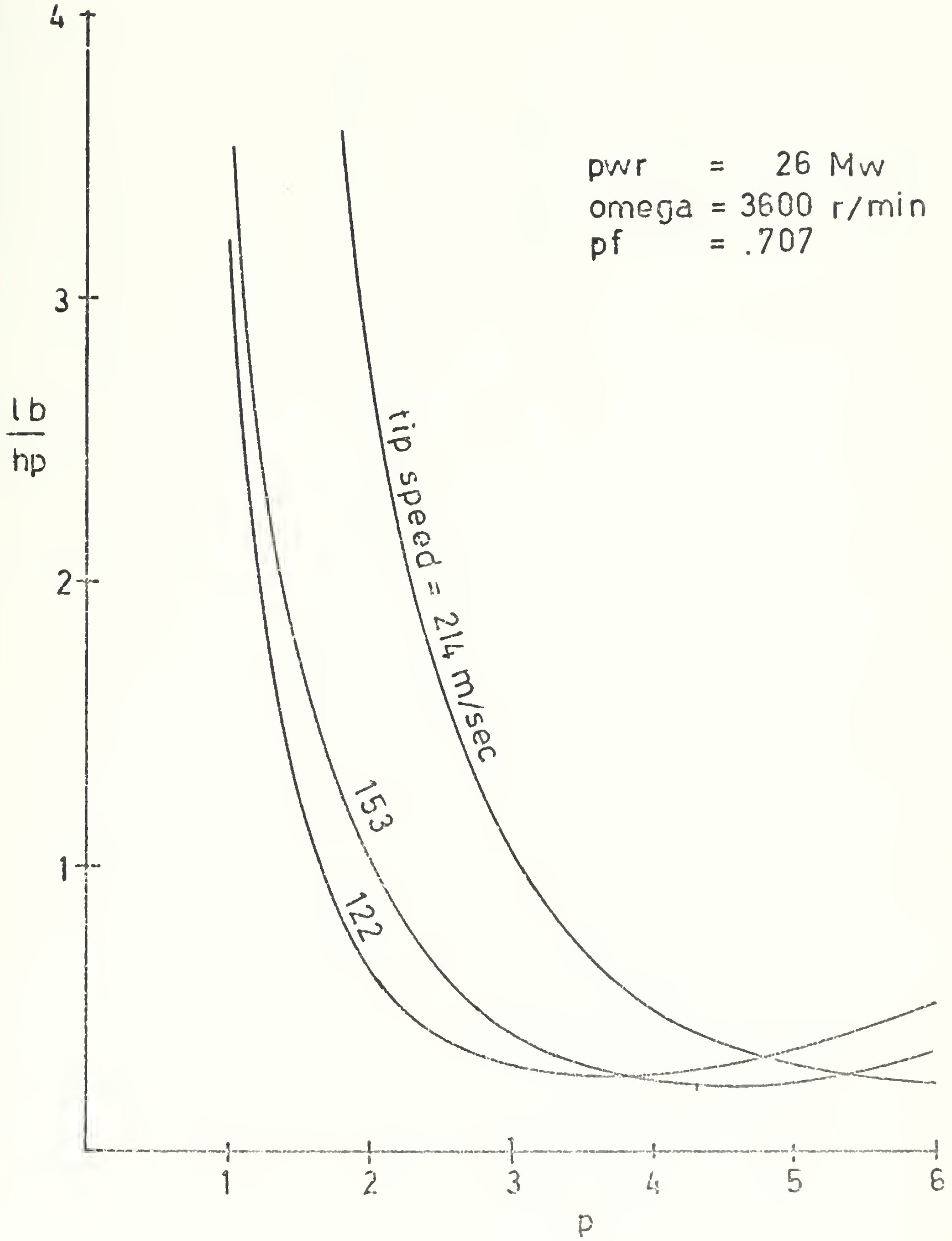

Figure 9

Motor Specific Weight

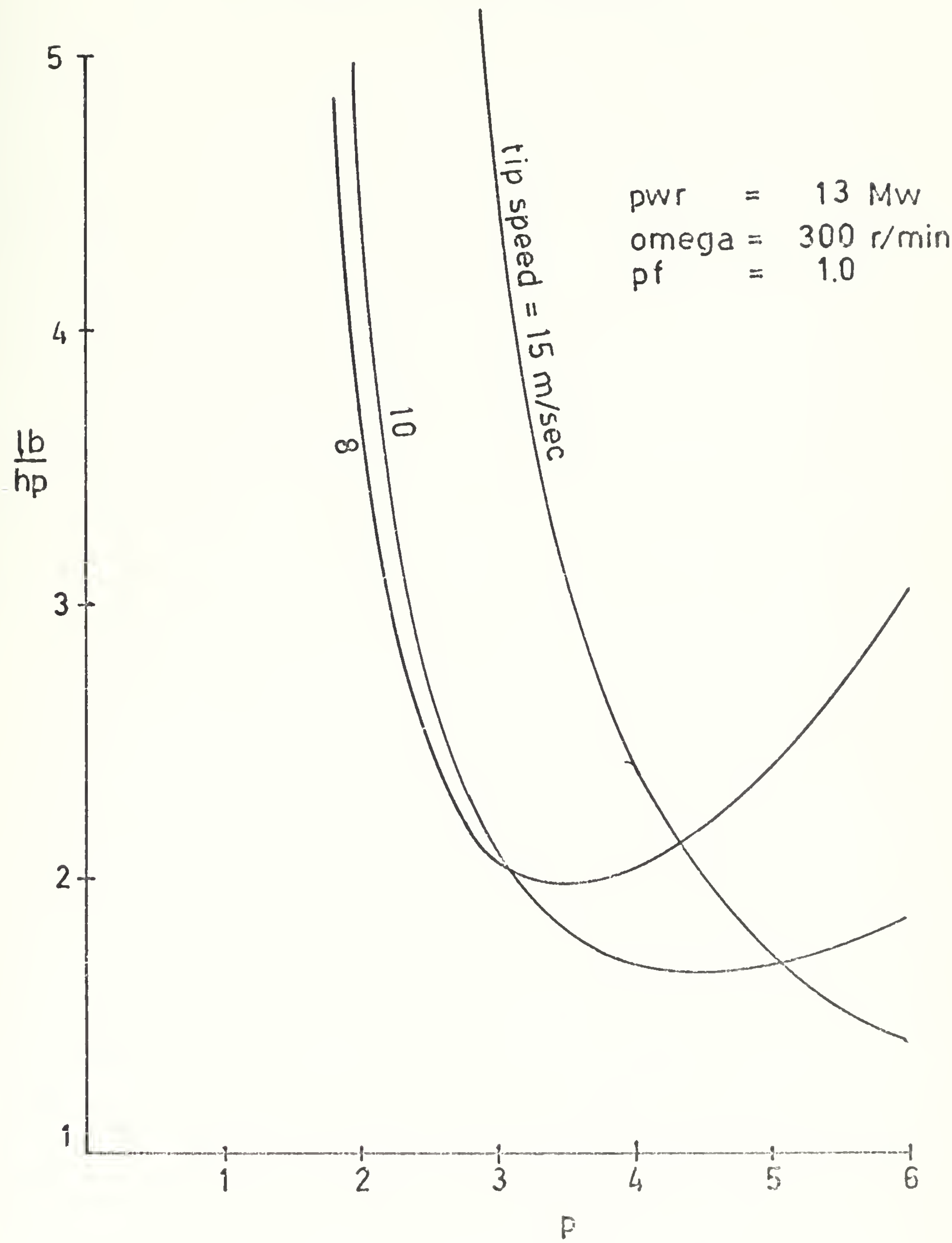

IV. DISCUSSION OF RESULTS

The most significant result of this study lies in the low values of specific weight (lb/hp) for superconducting machines. As indicated in Figure 8 specific weights on the order of 0.25 lb/hp* are theoretically possible in machines of the size typically found in marine propulsion plants.

The results of the study of direct-drive propulsion motors were less conclusive. It is apparent from Figure 9 that specific weights of 1.40 lb/hp are possible and that much lower specific weights are likely to be achieved in machines with larger numbers of poles and higher tip speeds. Nonetheless a specific weight of 1.40 is still an improvement over a conventional machine. This is evident from a comparison with the data for the propulsion motor in the USS Hunley, AS-31, given in Table 4.

hp	15,000
pole pairs	26
rpm	157
lb/hp	10.9

Table 4 Characteristics of Propulsion Motor of USS Hunley AS-31[11]

Consideration of the results of the generator designs indicates that in high speed machines, maximum tip speed will

*Compared to 4.0 lb/hp for conventional generators.

be a limit in machine design. However, this is not likely to be the case in lower speed machines such as the direct drive motor.

Machine characteristics such as low x_a and high efficiency are expected as a result of the smaller amount of armature winding required.

Aside from the significance of the data given for the various machine designs, there were two other notable results of this work. As described in the procedure for determining the field winding design (detailed in Appendix B), in order to reduce the number of variables involved it was assumed that the fields induced by the shield did not affect $B_{\rho max}$. However, the study conducted in Appendix E indicates that in some instances (especially for small values of p) this assumption is not warranted. From Figure 16 it is found that for the optimum generator design (x = .822, y = .848, p = 6) the error introduced is about one percent, whereas for the optimum motor (x = .801, y = .887, p = 6) the error is about .80 percent. These accuracies are expected to be much greater than the accuracy of the mathematical model being used.

Another result that became evident during the design study was that the linear interpolation technique used to find the minimum volume design (described in Appendix D) was not sufficiently accurate in all instances. Since the minima of the volume vs. R_o curve is quite broad for

$p = 1$ and 2, the linear interpolation yielded erroneous results in a few designs.

The accuracy of solution provided by the design program (within the limits imposed by the assumptions as discussed in Appendices B and E) is arbitrary. In the design study, a variation of 1% in output power was allowed. Likewise, in instances of solving for maximum flux density, the rate of change was required to be less than 10^{-4} at the calculated maximum. By changing these tolerences, the designer can obtain the accuracy desired in the solution.

V. CONCLUSIONS AND RECOMMENDATIONS

From the results of this study, the following can be concluded:

1. Superconducting electrical machines should provide considerable savings of weight and space in electrical propulsion systems.

2. The electrical efficiency of superconducting machines is substantially higher than the efficiency of conventional machines.

3. The solution of the design problem for a superconducting machine can be made at least as accurate as the design of a conventional machine.

4. High speed machines will be limited in speed of rotation by the maximum tip speed that can be sustained by the rotating parts.

5. An optimum design for a slow speed machine will require a large number of poles.

In the conduct of further investigation of the optimal design problem, or in application of the design program presented here, the following is recommended:

1. The body of data (array B(p, y)) representing the graph of $B_{\rho\,max}$/const. vs. y, should be expanded to account for larger values of p.

2. The design program should be modified to allow variation in VTIP. As indicated by Figures 8 and 9, an optimum machine design may occur for some value of VTIP

that is less than the maximum VTIP. By searching over a range of this variable, a numerical techniquo could easily be used to find the optimum design.

3. When a design is obtained, it is necessary to ensure that the error in $B_{\rho\ max}$, as described in Figures 13 to 16, is not excessive. It may be desirable to incorporate these figures in the design program, as was done with array B(p, y). It would then be possible to check each design within the program, making appropriate adjustment in the design parameters until a satisfactory result is obtained.

4. To ensure greater accuracy in the subroutine MIN, described in Appendix D, a false position solution technique[7] should be substituted for the linear interpolation method. A basic routine, such as the one presented on the following page, might be considered.

PROPOSED MODIFICATION TO SUBROUTINE MIN

```
            .
            .
            .
      RO(1)=OUTPT(1,3)
      RO(2)=OUTPT(J,3)
      DO 10 I=1,2
01    ROS=C1/(RO(I)**P)+RO(I)
      LT=PG*(RO(I)**(P-2))/CO
      X=RI/RO(I)
C     COMPUTE D(ROS**2)/DRO = A.
      A=-2*P*(C1**2)/(RO**(2*P+1))+2*C1*(1-P)/(RO**P)+2*RO
      IF(P-2)2,1,2
1     G=(-ALOG(X)+(1-X**4)/4)/4
      GO TO 3
2     G=(1-X**(2-P))/(4-P**2) + (1-X**(P+2))/((2+P)**2)
3     B=CO/G
      IF(P-2)5,4,5
C     COMPUTE DCO/DRO = C.
4     C=(B*(1+X**4))/(4*RO)
      GO TO 6
5     C=B*(X**(2-P)+X**(P+2))/(RO*(2+P))
C     COMPUTE DLT/DRO = D.
6     D=(P-2)*PG*(RO**(P-3))/CO - PG*C*(RO**(P-2))/(CO**2)+(2*PI)/(3*P)
C     COMPUTE DVOL/DRO = DVOL.
10    DVOL(I)=PI*LT*A + PI*(ROS**2)*D
      IF(STAR-1)11,12,12
11    DO 16 K=1,100
      STAR=1
      RO(3)=(RO(1)*DVOL(2))/(DVOL(2)-DVOL(1))+(RO(2)*DVOL(1))/(DVOL(1)
     1-DVOL(2))
```

```
      I=3
      GO TO 01
12    IF(ABS(DVOL(3))-1.E-04)17,17,13
13    IF(DVOL(3)*DVOL(2))14,17,15
14    RO(1)=RO(3)
      DVOL(1)=DVOL(3)
      GO TO 16
15    RO(2)=RO(3)
      DVOL(2)=DVOL(3)
16    CONTINUE
17    RO=RO(3)
```

THE SUBROUTINE RETURNS TO THE MAIN PROGRAM WITH THIS RO

APPENDIX A

Input Data

In organizing the machine program that was ultimately used, it was necessary to anticipate what information was likely to be available or fixed for the machine design. It was anticipated that certainly the desired power output would be known. The angular velocity of the rotor and power factor of the load may also be determined from particulars of the intended machine application. Further, it was expected that materials selection would precede this portion of a design, therefore various material characteristics will be available. Also expected is some knowledge of construction techniques to be employed, e.g. the type of armature cooling used and characteristics of the rotor design. Finally, some information concerning the dewar is necessary. Specifically the anticipated thickness of the dewar wall must be provided. Thus, input data will include:

a. power output, P_o

b. mechanical frequency, ω_m

c. maximum armature current density, J_a

d. dewar wall thickness, Δ

e. maximum tip speed of dewar, V_{tip}
(fixed by strength considerations in rotor design or limitations imposed by dewar technology)

f. power factor, pf

g. flux density to cause shield saturation, B_{rated}

h. average density of rotor, armature and shield, ρ_f, ρ_a, ρ_s

As mentioned in the Introduction, the superconducting material used in the field windings will have characteristic values of critical current and critical flux density. Therefore, additional input data will be a value of current density in the field windings, J_f, and the associated value of critical flux density, B_{max}.

For any field winding design, the geometry of the magnetic fields can be found. If J_f is known, the maximum flux density can be calculated. This maximum flux density must be found to ensure that it does not exceed the critical flux density associated with J_f (B_{max}).

Conversely, if J_f and B_{max} are given, certain limitations on field winding design are imposed.

It was found expedient to provide a body of data which could be used in the computer program for finding the best field winding design for some given J_f and B_{max}. The method for obtaining and utilizing this data is described in Appendix B.

APPENDIX B

Input Data for Field Winding Design

In the design of the field windings, three assumptions are made. First it is assumed that the fundamental component of the magnetic fields is the significant part. This assumption is fairly standard and has been shown to be acceptable.[6] Second, it is assumed that the fields generated by the armature may be neglected. Since the armature fields oppose the fields generated by the field windings, this approximation is conservative. Third, it is assumed that the fields reflected by the shield may be neglected. Although these fields add to those from the field winding, they are small, becoming insignificant as p increases. These approximations are made in order to decrease the number of variables in the calculations.

From Table I, it is seen that in the region $R_1 \angle \rho \angle R_2$ the maximum field intensity will be in the ρ-direction for $\phi = 0$. In accordance with the above approximations, for $p \neq 2$,

$$H_\rho = \frac{2J_f}{\pi(4-p^2)} \left[-2p + (2+p)\left(\frac{R_2}{\rho}\right)^{-p+2} - (2-p)\left(\frac{R_1}{\rho}\right)^{p+2} \right] \rho \qquad \text{(B-1)}$$

or

$$\frac{B}{\text{const.}} \equiv \frac{B_\rho \pi}{2\mu_o J_f R_2} = \frac{1}{(4-p^2)} \left[-2p \frac{\rho}{R_2} + (2+p)\left(\frac{\rho}{R_2}\right)^{p-1} - (2-p)y^{p+2} X \left(\frac{R_2}{\rho}\right)^{p+1} \right] \qquad \text{(B-2)}$$

If, for a given value of y,

$$\frac{d(B_{\rho}/\text{const.})}{d(\rho/R_2)} = 0 \qquad \text{(B-3)}$$

is solved for (ρ/R_2), and the value obtained used to evaluate Eq. (B-2), the maximum value of B_{ρ}/const. is obtained for that y.

For the case p = 2

$$H = \frac{2J_f}{\pi}\left[\frac{1}{4}\left(1-\frac{R_1^4}{\rho^4}\right) + \ln\frac{R_2}{\rho}\right]\rho \qquad \text{(B-4)}$$

and

$$\frac{B}{\text{const.}} \equiv \frac{B_{\rho}\pi}{2\mu_o J_f R_2} = \frac{1}{4}\left(\frac{\rho}{R_2} - y^4\left(\frac{R_2}{\rho}\right)^3\right) + \frac{\rho}{R_2}\ln\frac{R_2}{\rho}\,. \qquad \text{(B-5)}$$

Thus, if R_2 is known, it is possible to obtain

$$\frac{B_{\rho\,max.}}{J_f} = f(p,y). \qquad \text{(B-6)}$$

In the following computer program, for the IBM 1130, $B_{\rho\,max}$/const. is computed for values of p = 2 to 6 and y = 0.05 to 0.95. The results are displayed graphically in Figure 10. Using these results, it is possible to find the value of y corresponding to a given $B_{\rho\,max}$/const., thus fixing the radial dimensions of the field windings. The case p = 1 is not computed since for this value of p

$$B_{\rho\,max}/\text{const.} = 1-y. \qquad \text{(B-7)}$$

In the program, the following notation is used:

p = number of pole pairs

$y = R_1/R_2$, R_1 is the inside field radius, etc.

$R = \rho/R_2$, i.e. R1 in the program is the first value of ρ/R_2 and is not the inside field radius.

$B = B_\rho$/const.

B MAX = $B_{\rho\ max}$/const.

The program procedure is simply a solution of Eq. (B-3) and evaluation of Eq. (B-2) or Eq. (B-5) for the maximum value. For the case $p = 2$ a false position method[7] is used to solve Eq. (B-3), whereas the Newton-Raphson technique[8] is employed for all cases $p \neq 2$.

The printed results of this program include values of p, y and $B_{\rho\ max}$/const. which are used in the design program. The data represents the curves in Figure 10. Within the design program, $B_{\rho\ max}$/const. is computed, with which it is then possible to obtain from the curves a value of y which will satisfy the constraint imposed by the current and critical flux density.

The program used to solve for the data in the array B(p,y), and the subroutine used to interpret B(p,y) to find a value for y, are included in the following pages.

Figure 10

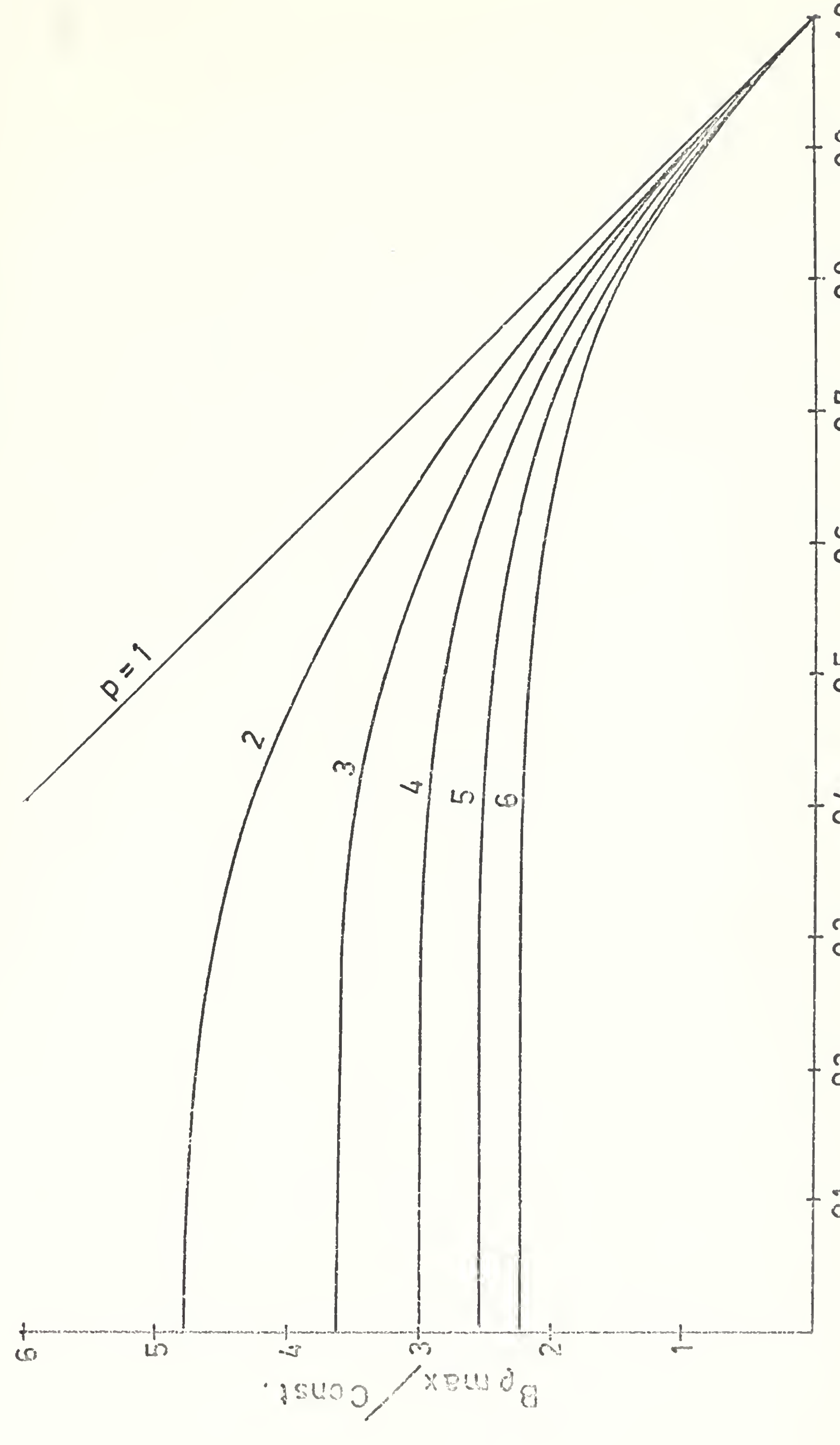

PROGRAM FOR DETERMINING DATA IN ARRAY B(P,Y)

```
// FOR
*IOCS (CARD,1132 PRINTER,DISK)
      INTEGER P
      DO 100 P=2,6
      DO 100 K=1,19
      Y=K*0.05
      IF(P-2)10,10,20
C     USE FALSE POSITION METHOD TO FIND RADIUS AT MAX RHO DIRECTED B
C     FOR CASE P=2.  NOTE, BPRIME=-.75+.75*(Y**4)/(R**4)+ALOG(R)=Y
10    R1=.40
      R2=1.0
      Y1=-.75 + .75*(Y**4)/(R1**4) - ALOG(R1)
      Y2=-.75 + .75*(Y**4)/(R2**4) - ALOG(R2)
      DO 14 N=1,100
      R3=(R1*Y2)/(Y2-Y1) + (R2*Y1)/(Y1-Y2)
      Y3=-.75 + .75*(Y**4)/(R3**4) - ALOG(R3)
C     CHECK FOR ADEQUATE CONVERGENCE
      IF(ABS(Y3) - 1.E-04)15,15,11
11    IF(Y2*Y3)12,15,13
12    R1=R3
      Y1=Y3
      GO TO 14
13    R2=R3
      Y2=Y3
14    CONTINUE
15    RNEW=R3
C     FIND MAX B FOR P=2
      BMAX=.25*RNEW - .25*(Y**4)/(RNEW**3) - RNEW*ALOG(RNEW)
      GO TO 90
C     USE NEWTON-RAPHSON METHOD TO FIND RADIUS AT MAX RHO DIRECTED B FOR
C     CASE P NOT EQUAL 2.
```

```
20    R=0.7
      DO 22 N=1,20
      A=(P**2+P-2)*(R**(2*P))-2*P*(R**(P+2))-(P**2-P-2)*(Y**(P+2))
      B=2*P*(P**2+P-2)*R**(2*P-1))-2*P*(P+2)*(R**(P+1))
      RNEW=R - A/B
C     CHECK CONVERGENCE
      IF(ABS(R - RNEW) - 1.E-04)23,23,21
21    R=RNEW
22    CONTINUE
C     FIND MAX B FOR P NOT EQUAL 2.
23    BMAX=((2+P)*(RNEW**(P-1)) - 2*P*RNEW - (2-P)*(Y**(P+2))/(RNEW**(P+
     11))))/(4 - P**2)
90    WRITE(3,91) P,Y,RNEW,BMAX
91    FORMAT(1H0,1I1,4X,1F4.2,3X,1F6.4,12X,1F6.4)
100   CONTINUE
      CALL EXIT
      END
// XEQ
// END
```

DATA READ TO THE MACHINE AS ARRAY B

.9500	.9000	.8500	.8000	.7500	.7000	.6500	.6000	.5500	.5000
.4500	.4000	.3500	.3000	.2500	.2000	.1500	.1000	.0500	.0000
.4723	.4721	.4711	.4686	.4637	.4556	.4439	.4283	.4090	.3861
.3597	.3302	.2976	.2623	.2243	.1838	.1411	.0961	.0490	.0000
.3599	.3599	.3598	.3595	.3585	.3563	.3524	.3461	.3369	.3243
.3082	.2885	.2650	.2379	.2071	.1727	.1347	.0932	.0483	.0000
.2962	.2962	.2962	.2962	.2959	.2953	.2940	.2914	.2869	.2799
.2699	.2565	.2393	.2181	.1928	.1631	.1291	.0907	.0476	.0000
.2533	.2533	.2533	.2533	.2533	.2531	.2526	.2516	.2494	.2456
.2394	.2303	.2177	.2011	.1802	.1546	.1241	.0883	.0470	.0000
.2220	.2220	.2220	.2220	.2220	.2219	.2217	.2213	.2203	.2183
.2145	.2084	.1991	.1862	.1689	.1468	.1193	.0860	.0464	.0000

SUBROUTINE PROGRAM FOR DETERMINING Y FROM ARRAY B

```
// FOR
      SUBROUTINE INTRP(Y)
      INTEGER P
      DIMENSION B(6,20), OUTPT(50,14)
      COMMON B, P, BC, C1, J, OUTPT, PI
      M=2
1     IF (B(P,M)-BC) 3, 4, 2
2     M=M+1
      GO TO 1
3     Q=(M-1)+(B(P,M-1)-BC)/(B(P,M-1)-B(P,M))
      Y=Q/20.
      GO TO 5
4     Y=M/20.
5     RETURN
      END
// DUP
*STORE      WS  UA  INTRP
```

APPENDIX C

Design Program

The design computer program, written for the IBM 1130, is an iterative solution of the basic design equations to find that machine design which requires the least volume.

The program uses the normalized variables x and y which represent the thickness of the armature and field windings. The variables R_2 and R_o serve to fix the radial location of the windings. The machine length is found from consideration of the working volume required to obtain the necessary internally generated power. The reduction from internal power to rated power is obtained from Eq. (II-15). The iterative procedure followed is based on varying values of R_o, which was found to be the most convenient parameter for this purpose.

Since

$$\text{Vol.} = \pi R_{os}^2 l_t \tag{C-1}$$

the variation of R_{os} with R_o was first examined. By evaluating Eq. (II-21) and substituting in Eq. (II-22) one obtains

$$R_{os} = \frac{4\mu_o J_f (1-y^{p+2}) \left(\frac{R_2}{R_o}\right)^{p+2} R_o^2}{\pi p B_{rated}(2+p)} + R_o \tag{C-2}$$

$$\equiv \frac{C_1}{R_o^p} + R_o \tag{C-3}$$

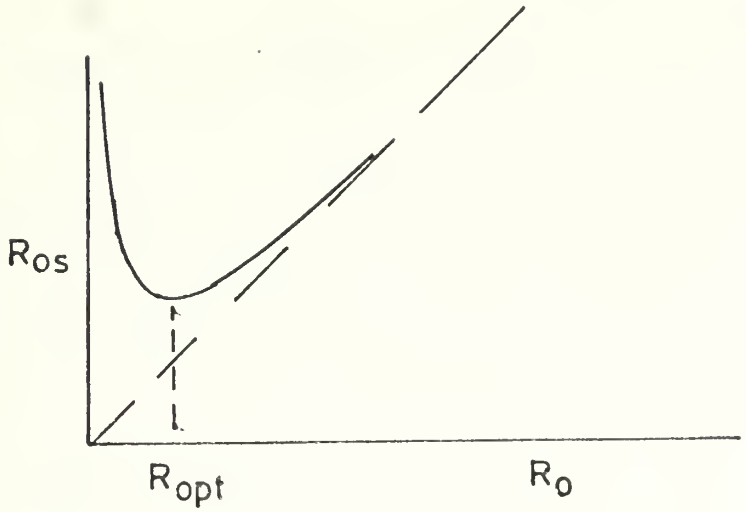

Figure 11 Variation of R_{os} with R_o

For small values of R_o, the shield is in the vicinity of intense magnetic fields and R_{os} must be large. As R_o increases, the thickness of the shield decreases but R_{os} is still larger than R_o. The value of R_o which requires the smallest R_{os} is found to be

$$R_{o\ opt.} = (pC_1)^{1/p+1} \tag{C-4}$$

Though this value of R_o does not necessarily yield a minimum volume machine (since no variation of l_t is considered), it is generally near the minimum volume value because of the significance of R_{os} in Eq. (C-1).

An R_o obtained from Eq. (C-4) will satisfy the constraint of Eq. (II-22). However, it must also satisfy Eq. (II-20).

Since

$$B_{max}(r=R_o) = \frac{4\mu_o J_f}{\pi(2+p)} \quad (1-y^{p+2}) \left(\frac{R_2}{R_o}\right)^{p+2} R_o \leq B_{rated} \qquad \text{(C-5)}$$

it is required that

$$R_o \geq (C_1/p)^{1/p+1}. \qquad \text{(C-6)}$$

Since

$$R^{p+1}_{o\ opt.} = pC_1 \geq \frac{C_1}{p} , \qquad \text{(C-7)}$$

Eq. (II-20) is also satisfied.

Turning now to the design program, the following procedure is carried out for successive values of p:

From the input data, one obtains

$$R_i = V_{tip}/\omega_m, \qquad \text{(C-8)}$$

$$R_2 = R_i - \Delta . \qquad \text{(C-9)}$$

Evaluating

$$B_{max}/\text{const.} = \frac{B_{rated}\ \pi}{2\mu_o J_f R_2} \qquad \text{(C-10)}$$

and entering the curves of B_{max}/const. vs. y, described in Appendix B, a value of y is obtained. With this information it is possible to evaluate C_1 and find $R_{o\ opt.}$ which is used to calculate an initial machine design.

Having selected a value for R_o one obtains

$$x = \frac{R_i}{R_o} . \qquad \text{(C-11)}$$

At this point in the program, the difference between the internally generated power and the desired power output is unknown. Assuming that this difference is largely due to load power factor, it is approximated that

$$P_g = P_o/pf \tag{C-12}$$

Since

$$P_g = \frac{3}{2} V_a I_a \tag{C-13}$$

$$= \frac{3}{2} \omega_e M I_f I_a \tag{C-14}$$

where

$$\omega_e = p\omega_m \tag{C-15}$$

$$I_f = \frac{\pi(1-y^2)R_2^2 J_f}{2N_f} \tag{C-16}$$

$$I_a = \frac{\pi(1-x^2)R_o^2 J_a}{6N_a} \tag{C-17}$$

and the appropriate expression for M is selected from Table II, one obtains

$$P_g = \frac{6\mu_o \omega_m J_a J_f}{\pi} (1-y^{p+2}) \left(\frac{R_2}{R_o}\right)^{p+2} l_m \; X$$

$$\left[\frac{1-x^{-p+2}}{4-p^2} + \frac{1-x^{p+2}}{(2+p)^2}\right] R_o^4 \tag{C-18}$$

for $p \neq 2$, or

$$P_g = \frac{3}{2} \frac{\mu_o \omega_m J_a J_f l_m}{\pi} (1-y^4) R_2^4 \cdot \left[\ln \frac{1}{x} + \frac{1-x^4}{4} \right] \tag{C-19}$$

for p = 2. From Eq. (C-18) or Eq. (C-19), it is possible to solve for l_m. Then, in accordance with Eq. (II-18) and Eq. (II-19),

$$l_t = l_m + \Delta l \tag{C-20}$$

$$= l_m + \frac{\pi}{3p} (1+x)R_o. \tag{C-21}$$

It is now possible to find the reduction in power from P_g to P_o. Applying the law of cosines to the diagram in Figure 5 results in

$$V_a^2 = V_t^2 + (x_s I_a)^2 - 2 V_t x_s I_a \cos (\frac{\pi}{2} + \theta). \tag{C-22}$$

Normalizing, one obtains

$$(V_t/V_a)^2 + x_a^2 - 2 V_t/V_a \, x_a \cos (\frac{\pi}{2} + \theta) - 1 = 0 \tag{C-23}$$

where

$$x_a = x_s \, I_a/V_a \tag{C-24}$$

is the per unit armature reactance loss. If Eq. (C-23) is solved for V_t/V_a, then Eq. (II-15) can be evaluated for P_o.

The value of P_o thus obtained is compared with the value specified in the input data. If the difference is greater than a given tolerance (1% of the desired value, for this program), the value of P_g assumed in Eq. (C-12)

is increased (or decreased) by the percentage difference between actual and desired output power (see statement 30 in the design program). The program then returns to Eq. (C-18) or Eq. (C-19), and calculation continues in this fashion until an acceptable difference is reached.

When a satisfactory P_o is obtained the program continues with calculation of

$$R_{os} = \frac{C_1}{R_o^p} + R_o \qquad \text{(C-3)}$$

$$\text{Vol.} = \pi R_{os}^2 \; l_t \qquad \text{(C-1)}$$

$$\text{Weight} = \pi l_t ((1-y^2)R_2^2 \; \rho_f + (1-x^2)R_o^2 \; \rho_a + (R_{os}^2 - R_o^2) \; \rho_s) \qquad \text{(C-25)}$$

$$V_t/N_a = V_t/V_a \cdot V_a/N_a = V_t/V_a \cdot$$

$$= \frac{24 \omega_m \mu_o l_m (1-y^{p+2}) R_2^{p+2} \; J_f}{\pi^2 (1-x^2) R_o^p} \; X$$

$$\left[\frac{1-x^{-p+2}}{4-p^2} + \frac{1-x^{p+2}}{(2+p)^2} \right] \qquad \text{(C-26)}$$

for $p \neq 2$, or

$$V_t/N_a = V_t/V_a \cdot \frac{6 \omega_m \mu_o l_m (1-y^4) R_2^4 \; J_f}{\pi^2 (1-x^2) R_o^2} \; X$$

$$(\ln \frac{1}{x} + \frac{1}{4} (1-x^4)) \qquad \text{(C-27)}$$

for p = 2, and

$$N_a I_a = \frac{\pi(1-x^2)R_o^2\ J_a}{6} \quad . \qquad \text{(C-28)}$$

The calculations described above are carried out for the initial value of R_o. The program continues by incrementing R_o (by 0.1 in this program), returning to Eq. (C-11) and repeating all the steps through Eq. (C-28). R_o continues to be incremented until it is found that the volume for successive designs is increasing, which indicates that the minimum volume design is within the range of those designs that have been completed. The program then calls a subroutine, described in Appendix D, which evaluates the data for the designs that have been completed, and from this data determines the minimum volume design.

Within the design program, the following notation is used:

PWR = desired P_o

POUT = actual P_o

B(p,y) = array of data representing the graphs in Figure 10

OUTPT = array in which parameters of each design are stored

BC = $B_{\rho\,max}$/const.

XA = un-normalized armature reactance, which becomes normalized when stored in OUTPT.

VAON = V_a/N_a

VTON = V_t/N_a

PG = P_g

ROS = R_{os}

VOL = Volume

WGT = Weight

NIA = $N_a I_a$

A print-out of the source deck for the design program is included in the following pages.

MAIN LINE PROGRAM

```
// FOR
*IOCS (CARD, TYPEWRITER, KEYBOARD, 1132 PRINTER, DISK)
      INTEGER P
      REAL JF, JA, PWR, MU, L, LM, LT, NIA
      DIMENSION B(6,20), OUTPT(50,14)
      COMMON B, P, BC, C1, J, OUTPT, PI
      READ (2,10) ((B(P,M), M=1,20), P=1,6)
10    FORMAT (10(F5.4,2X))
      DO 100 NO=1,3
      READ (2,11) VTIP, OMEGA, DELTA, BMAX, PFANG, BRATE, DENSF
11    FORMAT (7(F10.4))
      READ  (2,110) DENSA, DENSS, EPWR, EJF, EJA
110   FORMAT (5(F10.4))
      JF=EJF*(10.**8)
      JA=EJA*(10.**6)
      PWR=EPWR*(10.**6)
      PI=3.14159
      MU=(PI*4.0)/(10.**7)
      RI=VTIP/OMEGA
      R2=RI-DELTA
      DO 100 P=1,6
      WRITE (3,12) P, DELTA, JF, OMEGA, EPWR, JA, DENSF, VTIP, BMAX,
     1DENSA
12    FORMAT (1X , 'DATA', 20X, 'P = ', I1//1X,'DELTA = ',F5.3,' M',
     19X, 'JF = ', E8.2, ' A/M2', 8X, 'OMEGA = ', F4.0, ' RAD/SEC'//
     11X,'PWR = ',F6.1,' MW', 9X, 'JA = ', E8.2, ' A/M2', 8X, 'FLD DENSS
     1 = ', F5.0, ' KG/M3' //1X,'VTIP = ',F4.0,' M/SEC', 7X, 'B MAX = ',
     1F4.1, ' WEB/M2', 7X, 'ARM DENSS = ', F5.0, ' KG/M3'/)
      WRITE (3,13) PFANG, BRATE, DENSS
13    FORMAT (1X,'PF ANG = ',F5.3,' RAD',6X, 'B RATED = ', F4.1, ' WEB/
     1M2', 4X, 'SHL DENSS = ', F5.0, ' KG/M3'//1X,'DESIGN PARAMETERS'//
     13X,'X',5X,'Y',4X,'RO',3X,'ROS',4X,'LT',4X,'XA',3X,'VT/N',5X,'NIA',
```

```
     16X,'POUT',3X,'VOL',5X,'WGT',5X,'VI'/13X,'(M)',3X,'(M)',3X,'(M)',
     11X,'(P.U.)(V/TURN)(A-TURNS)',3X,'(MW)',2X,'(M3)',4X,'(KG)',4X,
     1'(MW)'/)
      U=P
C     COMPUTE BMAX/CONST. (BC)
      BC=(BMAX*PI)/(2*JF*MU*R2)
C     WITH BMAX/CONST, DETERMINE ALLOWABLE Y.
      CALL INTRP(Y)
      C1=(4*MU*JF*(1-Y**(P+2))*(R2**(P+2)))/(P*PI*BRATE*(2+P))
      J=1
      FLAG=0
      STAR=0
C     START WITH THE VALUE OF RO TO GIVE A MINIMUM ROS.
      EXP=1./(U+1.)
      RO=(U*C1)**EXP
20    X=RI/RO
C     TO ACCOUNT FOR POWER FACTOR ASSUME
      PG=PWR/COS(PFANG)
      IF (P-2) 22, 21, 22
21    A=(-ALOG(X)+(1-X**4)/4)/4
      GO TO 23
22    A=(1-X**(2-P))/(4-P**2) + (1-X**(P+2))/((2+P)**2)
23    CO=(6*MU*OMEGA*JA*JF*(1-Y**(P+2))*(R2**(P+2))*A)/PI
      DO 300 N=1,15
      LM=PG*(RO**(P-2))/CO
      DL=(PI*(1+X)*RO)/(3*P)
      LT=LM+DL
C     COMPUTE THE ARMATURE LOSS. (XA)
      IF (P-2) 26, 25, 26
25    D=(1-X**4)/4+(X**4)*ALOG(X)+((1-X**4)**2)/8
      XA=(6*MU*OMEGA*LT*(RO**2)*JA*D)/((PI**2)*(1-X**2))
      GO TO 27
26    D=(P-2)-(P+2)*(X**4)+(4*(X**(P+2)))+2*(P-2)*((1-X**(P+2))**2)/
     1(P+2)
      XA=(6*MU*OMEGA*LT*(RO**2)*JA*D)/((PI**2)*(P**2-4)*(1-X**2))
```

```
27    VAON=(24*MU*OMEGA*LM*(1-Y**(P+2))*(R2**(P+2))*JF*A)/((PI**2)*(1-
     1X**2)*(RO**P))
C     FROM THE LAW OF COSINES, GET A QUADRATIC TO SOLVE FOR THE VOLTAGE
C     LOSS IN THE ARMATURE REACTANCE. (VT/VA = VTOVA)
      E=-(2*XA*COS(PI/2+PFANG))/(VAON)
      F=(XA**2)/(VAON**2)-1
      DISC=(E**2)-(4*F)
      S=SQRT(DISC)
      VTOVA=(-E+S)/2
C     DETERMINE THE ACTUAL POWER OUTPUT.
      POUT=PG*VTOVA*COS(PFANG)
      IF (ABS(POUT-PWR)-.01*PWR) 31,31,30
30    PG=PG*(1-(POUT-PWR)/PWR)
300   CONTINUE
C     IF THE ACTUAL POWER OUTPUT IS SUFFICIENTLY CLOSE TO THE DESIGN
C     VALUE, COMPLETE THE COMPUTATION OF DESIGN PARAMETERS AND STORE.
31    ROS=C1/(RO**P)+RO
      VOL=PI*(ROS**2)*LT
      WGT=PI*LT*((1-Y**2)*(R2**2)*DENSF + (1-X**2)*(RO**2)*DENSA  +
     1((ROS**2-RO**2))*DENSS)
      VTON=(VTOVA)*(VAON)
      NIA=(PI*(1-X**2)*(RO**2)*JA)/6
      OUTPT (J,1) = X
      OUTPT (J,2) = Y
      OUTPT (J,3) = RO
      OUTPT (J,4) = ROS
      OUTPT (J,5) = LT
      OUTPT (J,6) = XA/VTON
      OUTPT (J,7) = VTON
      OUTPT (J,8) = NIA
      OUTPT (J,9) = POUT*1.0E-06
      OUTPT (J,10) = VOL
      OUTPT (J,11) = WGT
      OUTPT (J,12) = PG*1.0E-06
      OUTPT (J,13) = CO
      OUTPT (J,14) = A
```

```
C     STAR SIGNALS THAT THE DESIGN JUST COMPLETED WAS THE MINIMUM
C     VOLUME DESIGN.
      IF (STAR-1) 40, 90, 90
40    IF (J-1) 44, 44, 41
41    IF (OUTPT(J,10)-OUTPT(J-1,10)) 45, 45, 42
C     FLAG SIGNALS THAT A SUFFICIENT NUMBER OF DESIGNS (2) BEYOND THE
C     MINIMUM VOLUME DESIGN HAVE BEEN COMPLETED.
42    IF (FLAG-2) 43, 47, 47
43    FLAG=FLAG+1
      GO TO 45
44    K=10.*RO
      G=K
      RO=G/10.
C     RO IS INCREMENTED BY .01 FOR EACH SUCCESSIVE DESIGN.
45    RO=RO+.10
46    J=J+1
      GO TO 20
47    CALL MIN(RO)
      STAR=1
      GO TO 46
90    JO=J
      J=1
91    WRITE (3,92) OUTPT (J,1), OUTPT (J,2), OUTPT (J,3), OUTPT (J,4),
     1OUTPT (J,5), OUTPT (J,6), OUTPT (J,7), OUTPT (J,8), OUTPT (J,9),
     1OUTPT (J,10), OUTPT (J,11), OUTPT (J,12)
92    FORMAT (6(F5.3,1X),F6.0,2X,E8.2,1X,F6.1,1X,F6.3,1X,F7.0,1X,F6.1/)
      J=J+1
      IF (JO-J) 100, 94, 91
94    WRITE (3, 95)
95    FORMAT (1X,'MINIMUM VOLUME DESIGN'/)
      GO TO 91
100   CONTINUE
      CALL EXIT
      END
// XEQ
// END
```

APPENDIX D

Subroutine to Find the Minimum Volume Design

After the design program computes three designs of successively increasing volume, it calls the subroutine MIN. The data stored in OUTPT at this time will include at least two designs beyond the minimum volume design.

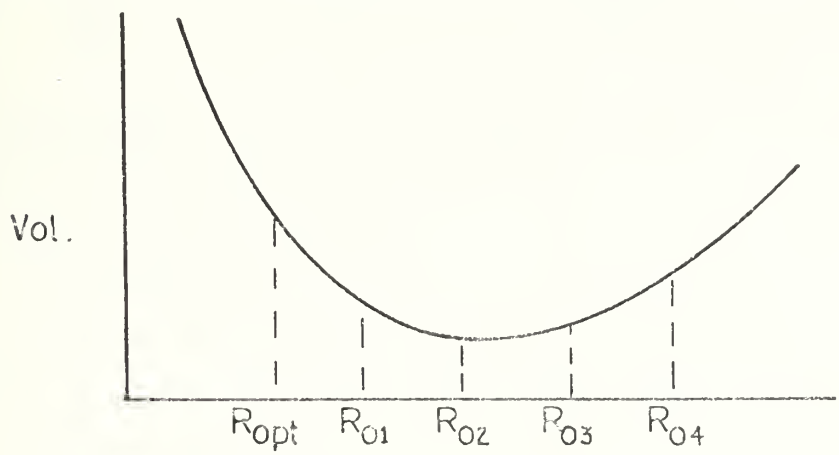

Figure 12a Data Stored in OUTPT

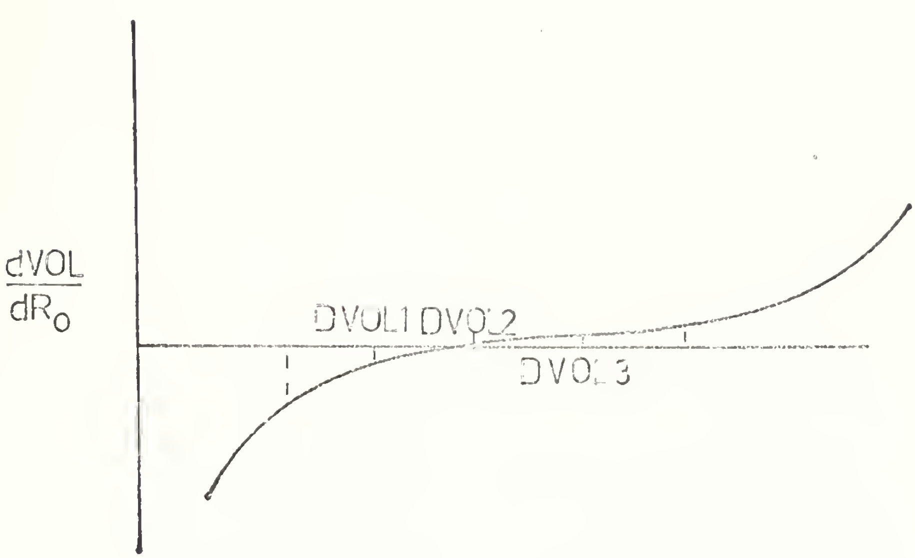

Figure 12b Points Calculated by MIN

The program computes $dVol/dR_o$ for the three values of R_o that bracket the minimum volume design.

Since

$$Vol = \pi R_{os}^2 \; l_t \qquad (D\text{-}1)$$

then

$$\frac{dVol}{dR_o} = \pi R_{os}^2 \frac{dl_t}{dR_o} + \pi l_t \frac{d(R_{os}^2)}{dR_o} . \qquad (D\text{-}2)$$

Considering Equations (C-18), (C-19), and (C-21), it is possible to express

$$l_t = \frac{P_g}{C_o} R_o^{p-2} + \frac{\pi}{3p} (R_o + R_i) \qquad (D\text{-}3)$$

where

$$C_o = f(x). \qquad (D\text{-}4)$$

Therefore

$$\frac{dl_t}{dR_o} = (p-2) \frac{P_g}{C_o} R_o^{p-3} - \frac{P_g}{C_o^2} \frac{dC_o}{dR_o} R_o^{p-2} + \frac{\pi}{3p} \qquad (D\text{-}5)$$

and, from Eq. (C-3),

$$\frac{d(R_{os}^2)}{dR_o} = -2pC_1^2 R_o^{-2p-1} + 2C_1(1-p)R_o^{-p} + 2R_o . \qquad (D\text{-}6)$$

When values of DVOL for R_{01}, R_{02} and R_{03} have been computed, linear interpolation is used to find the value of R_o for which DVOL $(R_o) = 0$. Control then returns to the main design program where the design characteristics for this value of R_o are found.

A print-out of the source deck for this sub-routine is included in the follwoing pages.

SUBROUTINE PROGRAM FOR DETERMINING RO FOR MINIMUM
VOLUME DESIGN

```
// FOR
      SUBROUTINE MIN(RO)
      INTEGER P
      REAL LT
      DIMENSION OUTPT(50,14), G(6,20), DVOL(3)
      COMMON G, P, BC, C1, J, OUTPT, PI
      IF (P-2) 15, 15, 16
16    K=J
      IF (J-4) 1, 1, 2
1     K=5
2     DO 10 KO=1,3
      RO=OUTPT (K-4,3)
      ROS=OUTPT (K-4,4)
      LT=OUTPT (K-4,5)
      PG=OUTPT (K-4,12)*1.0E 06
      X=OUTPT (K-4,1)
      CO=OUTPT(K-4,13)
C     COMPUTE D(ROS**2)/DRO = A.
      A=-2*P*(C1**2)/(RO**(2*P+1))+2*C1*(1-P)/(RO**P)+2*RO
      B=CO/OUTPT(K-4,14)
      IF (P-2) 8, 7, 8
C     COMPUTE DCO/DRO = C.
7     C=(B*(1+X**4))/(4*RO)
      GO TO 9
8     C=B*(X**(2-P)+X**(P+2))/(RO*(2+P))
C     COMPUTE DLT/DRO = D.
9     D=(P-2)*PG*(RO**(P-3))/CO - PG*C*(RO**(P-2))/(CO**2)+(2*PI)/(3*P)
C     COMPUTE DVOL/DRO = DVOL.
      DVOL(KO)=PI*LT*A + PI*(ROS**2)*D
      K=K+1
10    CONTINUE
```

```
C      AFTER DVOL IS COMPUTED FOR THE THREE DESIGNS THAT BRACKET THE
C      MINIMUM VOLUME DESIGN, LINEAR INTERPOLATION IS USED TO FIND RO FOR
C      THE MINIMUM VOLUME DESIGN.
       IF (DVOL(1)*DVOL(2)) 11, 13, 12
11     RO=OUTPT (J-4,3)+(DVOL (1)*(OUTPT (J-3,3)-OUTPT (J-4,3)))/(DVOL (1
      1)-DVOL (2))
       GO TO 14
12     RO=OUTPT (J-3,3)+(DVOL (2)*(OUTPT (J-2,3)-OUTPT(J-3,3)))/(DVOL (2
      1)-DVOL (3))
       GO TO 14
13     RO = OUTPT (J-3,3)
       GO TO 14
15     RO=OUTPT (1,3)
14     RETURN
       END
// DUP
*STORE      WS  UA  MIN
```

APPENDIX E

Effect of the Shield on Maximum Flux Density

As described in Appendix B, the assumption was made, in determining characteristics of the field windings, that the effect of the shielding could be neglected. The significance of this assumption is examined as follows:

If B_ρ /const. is computed, as in Appendix B, without neglecting shield effect, the result is

$$\frac{B_\rho}{\text{Const.}} = \frac{1}{(4-p^2)} \left[-2p \left(\frac{\rho}{R_2}\right) + (2+p) \left(\frac{\rho}{R_2}\right)^{p-1} - (2-p) y^{p+2} \times \left(\frac{R_2}{\rho}\right)^{p+1} + (2-p)(1-y^{p+2}) \left(\frac{R_2}{R_o}\right)^{2p} \left(\frac{\rho}{R_2}\right)^{p-1} \right] \tag{E-1}$$

for $p \neq 2$, and

$$\frac{B}{\text{Const.}} = \left[\frac{1}{4}\left(\frac{\rho}{R_2} - y^4 \left(\frac{R_2}{\rho}\right)^3 \right) + \frac{\rho}{R_2} \ln \frac{R_2}{\rho} + \frac{1}{4}(1-y^4) \times \left(\frac{R_2}{R_o}\right)^4 \frac{\rho}{R_2} \right] \tag{E-2}$$

Recognizing that

$$\frac{R_2}{R_o} = \frac{R_i - \Delta}{R_o} = x - \delta \tag{E-3}$$

where

$$\delta = \frac{\Delta}{R_o} \tag{E-4}$$

Eq. (E-1) and Eq. (E-2) can be written in terms of the normalized parameters x, y and δ .

Assuming that δ is constant over a range of machine sizes, it is possible to compute the actual $B_{\rho\ max}$/const. in terms of x and y. The solution technique is the same as that described in Appendix B. One can then compare the value of $B_{\rho\ max}$/const. obtained from the simplified equations with that value obtained from the method described above.

The results of such a comparison are displayed in the following graphs. The data is for the cases of p = 3 to 6, which are of most interest.

Figure 13

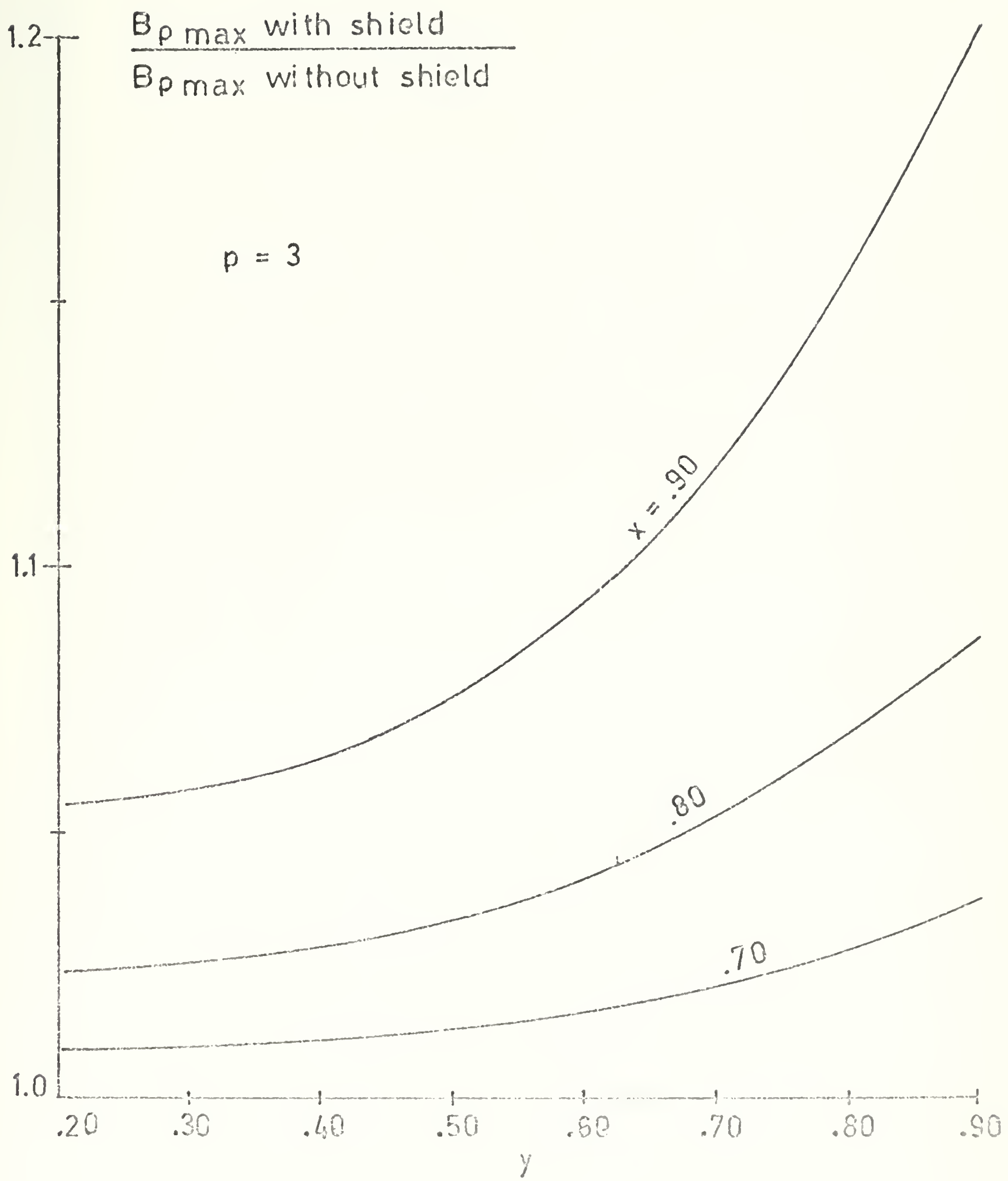

$\frac{B_{\rho\,max} \text{ with shield}}{B_{\rho\,max} \text{ without shield}}$
p = 3
x = .90
.80
.70
1.2
1.1
1.0
.20
.30
.40
.50
.60
.70
.80
.90
y

Figure 14

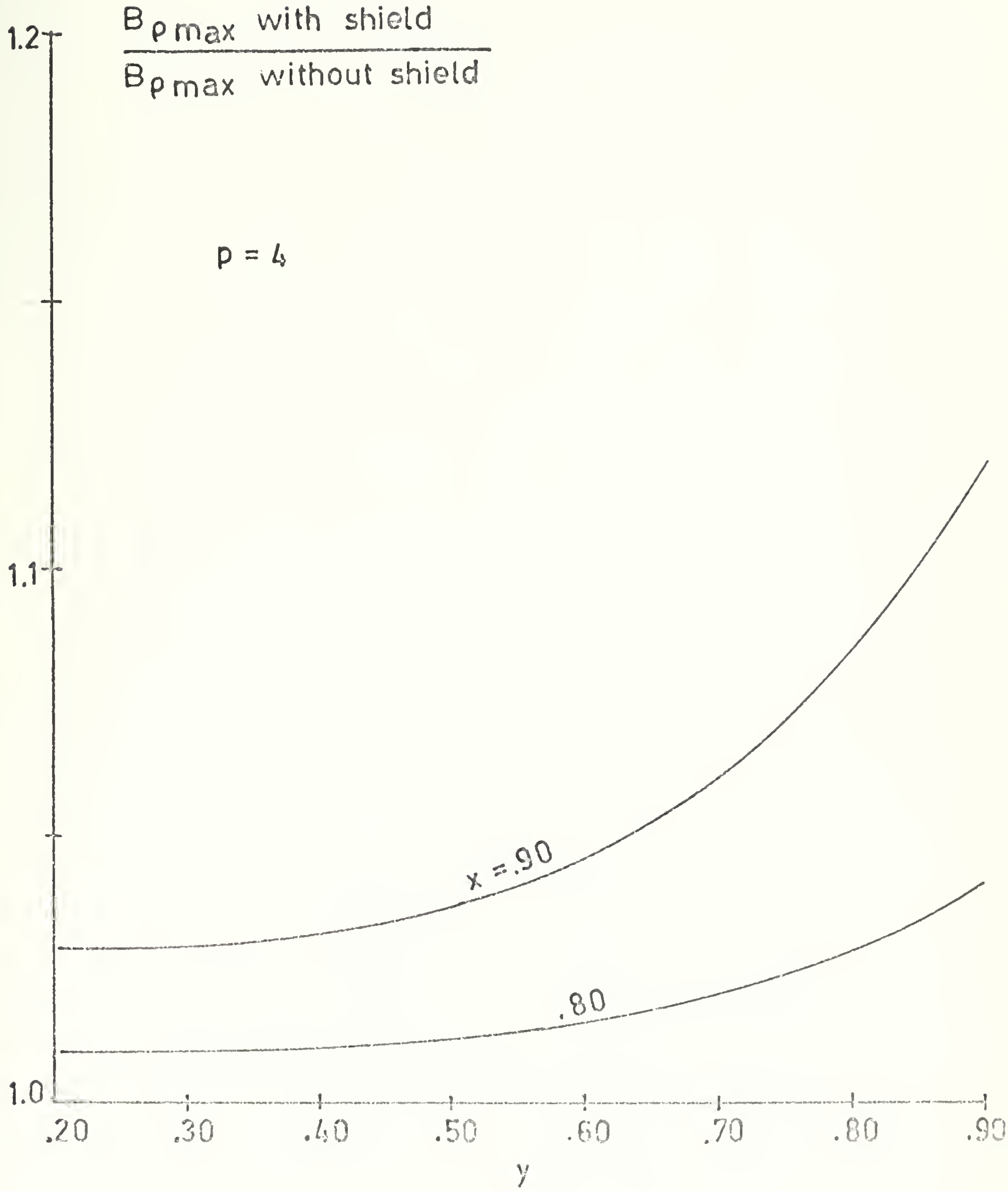

$\frac{B_{\rho\,max} \text{ with shield}}{B_{\rho\,max} \text{ without shield}}$
1.2
1.1
1.0
p = 4
x = .90
.80
.20
.30
.40
.50
.60
.70
.80
.90
y

Figure 15

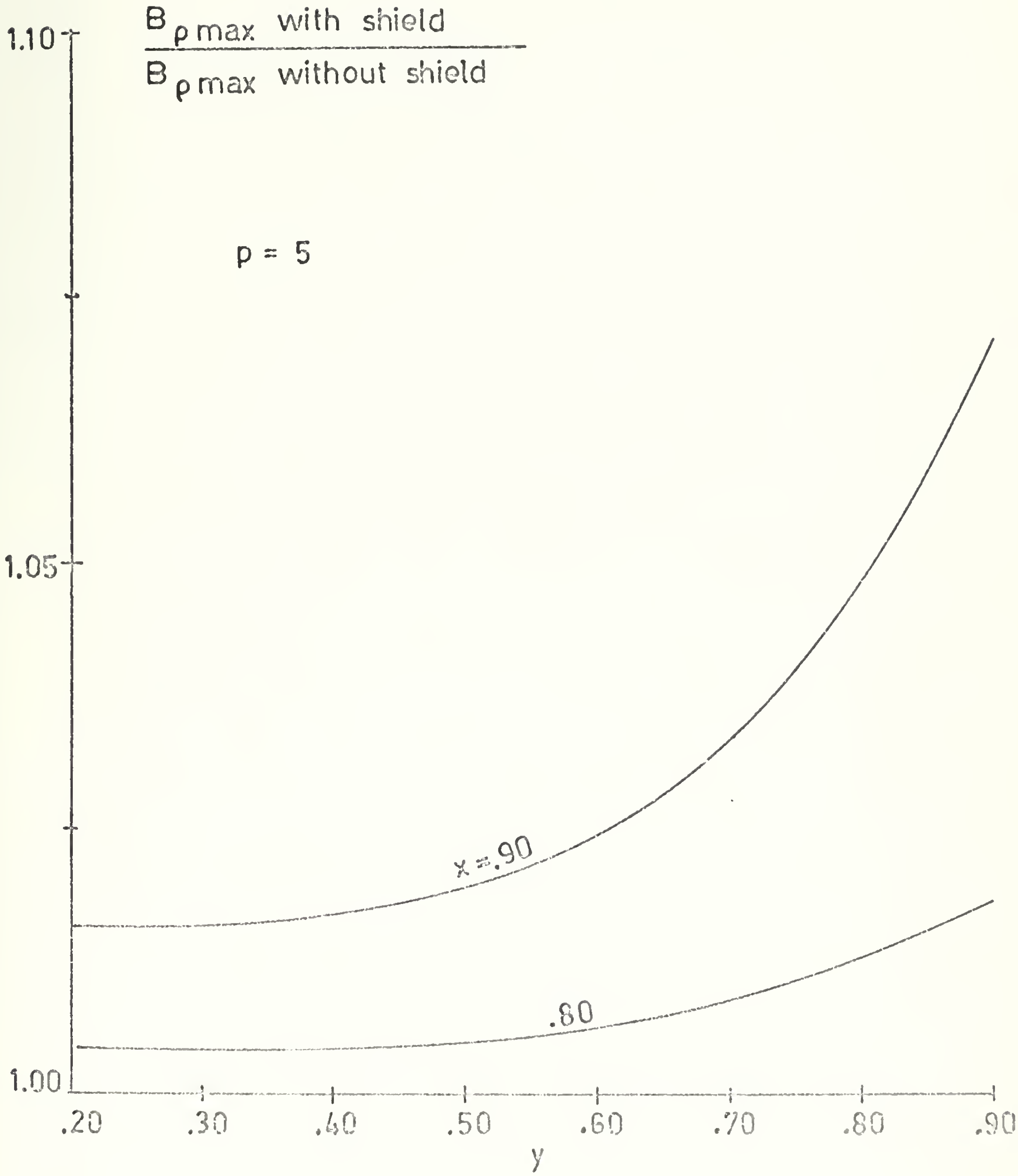

$\frac{B_{\rho\,max} \text{ with shield}}{B_{\rho\,max} \text{ without shield}}$
1.10
1.05
1.00
p = 5
x = .90
.80
.20
.30
.40
.50
.60
.70
.80
.90
y

Figure 16

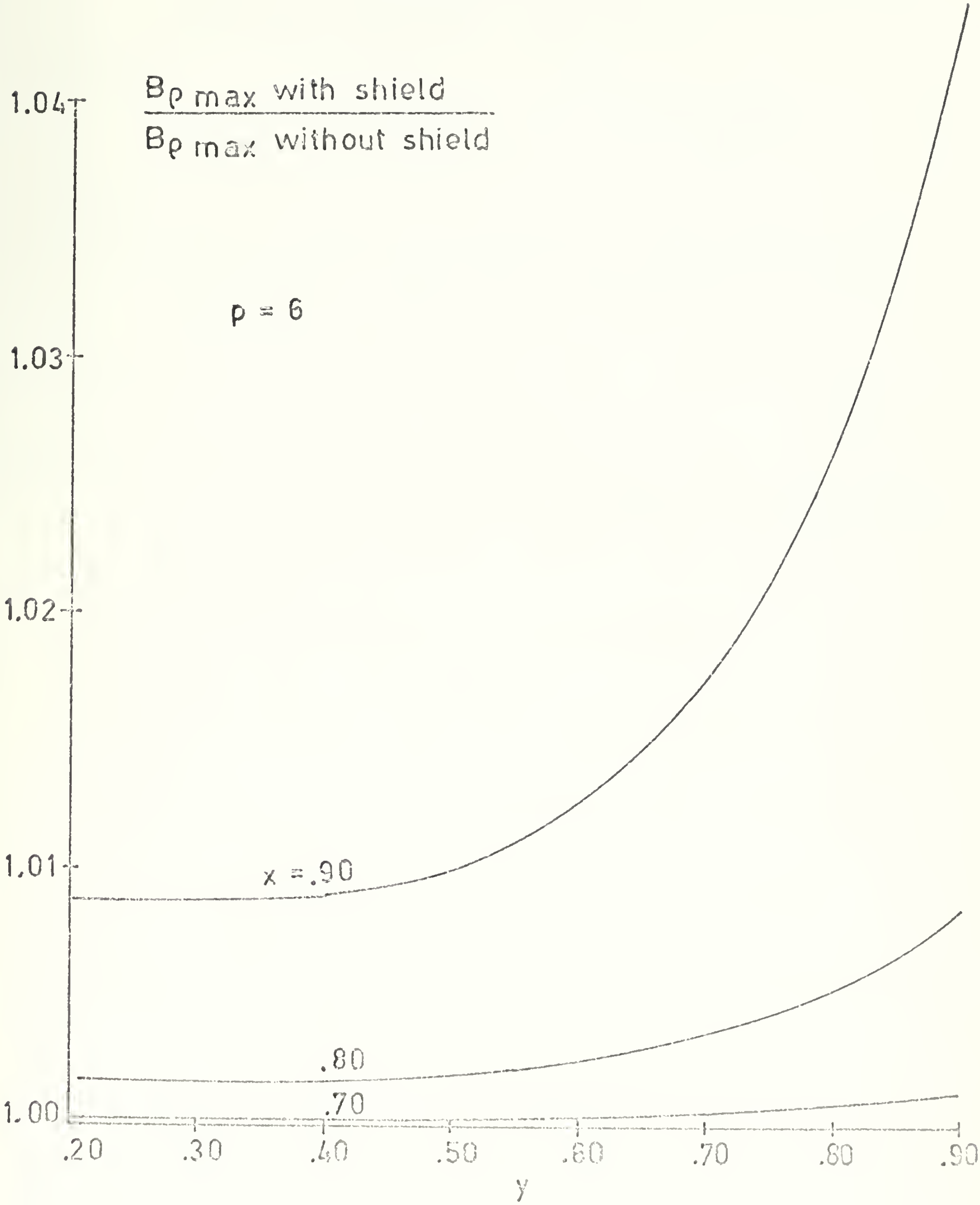
$\frac{B_{\rho\,max} \text{ with shield}}{B_{\rho\,max} \text{ without shield}}$
p = 6
1.04
1.03
1.02
1.01
1.00
x = .90
.80
.70
.20
.30
.40
.50
.60
.70
.80
.90
y

BIBLIOGRAPHY

1. Sibley, E. H., Frankel, E. G., Reynolds, J. M., "Superconductivity: Status and Implications for Marine Applications", Paper No. 8, Symposium on Marine Power Plants, Society of Naval Architects and Marine Engineers, (May 1966).

2. Matjasko, L. S., "Control of Superconducting Machines for Ship Propulsion", S.M. Thesis, Naval Architecture, Massachusetts Institute of Technology, 1968.

3. Janes, C. F., "Superconductors for Shipboard Power Applications", Paper presented at Fourth Annual Technical Symposium of Association of Senior Engineers of Naval Ships System Command", (March 1966)

4. Rissick, H., The Fundamental Theory of Arc Converters, London: Chapman and Hall, 1939.

5. Avco-Everett Research Laboratory, Research and Design of Superconductive and Cryogenic Electronic Power Generator, Final Technical Report Contract No. DA-44-009-AMC-236(T), Everett, Mass., (January 1965).

6. Woodson, H. H., Stekly, Z. J. J., Halas, E., "A Study of Alternators with Superconducting Field Windings", I.E.E.E. Transactions, PAS-85 (March 1966).

7. McCracken, D. D., Dorn, W. S., Numerical Methods and Fortran Programming, New York, Wiley, 1965.

8. McCracken, D. D., A Guide to Fortran IV Programming, New York, Wiley, 1965.

9. Treshchev, I. I., "O Nyekotroikh Osobyennostyakh Sinkhronnoi Mashini so Sverkhprovodyashchai Obmotkoi Vozboozhdeniya", Elektrichestvo II, 1967.

10. Voldek, A. I., "Osnovi Metodiki Rascheta Magnitnikh Pulyai Lobovikh Chastyai Obmotok Elektricheskikh Mashin", Elektrichestvo I, 1963.

11. Burford, H. M., Kock, R. L., Westbrook, J. D., "Performance of a Diesel Electric A.C. Propulsion Plant", Hampton Roads Section, Society of Naval Architects and Marine Engineers, (October 1962)